

5
CLASSIFICATION CANCELLED

UNAVAILABLE

RM No. E6J14

UNAVAILABLE

NACA

LANGLEY AIR FORCE LIBRARY

RESEARCH MEMORANDUM

for the

Air Materiel Command, Army Air Forces

ALTITUDE-WIND-TUNNEL INVESTIGATION OF PERFORMANCE OF SEVERAL
PROPELLERS ON YP-47M AIRPLANE AT HIGH BLADE LOADING

II - CURTISS 838-1C2-18R1 FOUR-BLADE PROPELLER

By Lewis E. Wallner and Solomon M. Sorin

Aircraft Engine Research Laboratory
Cleveland, Ohio

*Made Unavailable by
Admin. Action per
Hdgr. Let. dtd
6-8-59 /BAM.*

CLASSIFIED DOCUMENT

This document contains classified information affecting the National Defense of the United States within the meaning of the Espionage Act, USC 5041 and 5042. Its transmission or the revelation of its contents in any manner to an unauthorized person is prohibited by law. Information so classified may be inserted only to persons in the military and naval services of the United States, appropriate civilian officials and employees of the Federal Government who have a legitimate interest therein, and to United States citizens of known loyalty and discretion who of necessity must be informed thereof.

NOV 26 1946

**NATIONAL ADVISORY COMMITTEE
FOR AERONAUTICS**

WASHINGTON

**LANGLEY RESEARCH AERONAUTICAL
LABORATORY**

NOT TO BE TAKEN FROM THIS ROOM

6

UNAVAILABLE



UNAVAILABLE

NATIONAL ADVISORY COMMITTEE FOR AERONAUTICS

RESEARCH MEMORANDUM

for the

Air Materiel Command, Army Air Forces

ALTITUDE-WIND-TUNNEL INVESTIGATION OF PERFORMANCE OF SEVERAL

PROPELLERS ON YP-47M AIRPLANE AT HIGH BLADE LOADING

II - CURTISS 838-1C2-1SR1 FOUR-BLADE PROPELLER

By Lewis E. Wallner and Solomon M. Sorin

SUMMARY

An investigation was conducted in the Cleveland altitude wind tunnel to determine the performance of a Curtiss propeller with four 838-1C2-1SR1 blades on a YP-47M airplane at high blade loadings and engine powers. The study was made for a range of power coefficients between 0.30 and 1.00 at free-stream Mach numbers of 0.40 and 0.50. The results of the force measurements indicate primarily the trend of propeller efficiency for changes in power coefficient or advance-diameter ratio, inasmuch as corrections for the effects of tunnel-wall constriction on the installation have not been applied. Slipstream pressure surveys across the propeller disk are presented to illustrate blade thrust load distribution for several operating conditions.

At a free-stream Mach number of 0.40, nearly constant peak efficiencies were obtained at power coefficients from 0.30 to 0.70. A change in power coefficient from 0.70 to 0.90 reduced the peak efficiency about 5 percent. Blade stall at the tip sections became evident for a power coefficient of 0.91 when the advance-diameter ratio was reduced to 1.67.

At a free-stream Mach number of 0.50, the highest propeller efficiencies were obtained for power coefficients from 0.80 to 1.00 at advance-diameter ratios above 2.90. At advance-diameter ratios below 2.90, the highest efficiencies were obtained for power coefficients of 0.60 and 0.70. The envelope of the efficiency curves decreased about 12 percent between advance-diameter ratios of 2.60 and 4.20. Local compressibility effects became evident for a power coefficient of 0.40 when the advance-diameter ratio was decreased to 1.75.

UNCLASSIFIED

UNAVAILABLE

In general, the thrust loading on the outboard sections increased more rapidly than on the inboard sections as the power coefficient was increased or as the advance-diameter ratio was decreased. For conditions where blade stall or compressibility effects were evident the thrust loading on the tip sections decreased and a portion of the load shifted to the inboard sections.

INTRODUCTION

An investigation of the performance of several propellers on the YP-47M airplane at high blade loadings has been conducted in the Cleveland altitude wind tunnel at the request of the Air Materiel Command, Army Air Forces. As part of the program, a study was made of a Curtiss 838-1C2-18R1 four-blade propeller. The results and a brief discussion of the characteristics of this propeller are presented.

The investigation was made for a range of power coefficients between 0.30 and 1.00 at free-stream Mach numbers of 0.40 and 0.50, density altitudes from 20,000 to 45,000 feet, engine powers from 150 to 2500 brake horsepower, and engine speeds from 1100 to 2900 rpm. The propeller efficiencies, as in reference 1, were determined from force measurements; blade thrust distribution was obtained from pressure surveys in the propeller slipstream.

PROPELLER AND POWER PLANT

Propeller	
Hub	CS42S-B40
Blade design	Curtiss 838-1C2-18R1
Number of blades	four
Blade sections	NACA 16 series
Propeller diameter	13 feet
Activity factor ¹	120
Propeller gear ratio	20:9
Engine	R-2800-73
War emergency power rating:	
Engine speed, rpm	2800
Manifold pressure, in. Hg	72.0
Brake horsepower	2800
Military power rating:	
Engine speed, rpm	2800
Manifold pressure, in. Hg	53.5
Brake horsepower	2100

Normal power rating:

Engine speed, rpm	2600
Manifold pressure, in. Hg	41.5
Brake horsepower	1700

¹The activity factor is a nondimensional function of the propeller plan form designed to express the integrated capacity of the propeller blade elements for absorbing power (reference 1).

The propeller blade-form characteristics are given in figure 1. The Curtiss 838-1C2-18R1 propeller blade is shown in figure 2.

APPARATUS AND METHODS

The assembled propeller as installed on the YP-47M airplane in the 20-foot diameter test section of the altitude wind tunnel is shown in figure 3. The test equipment is described in reference 1.

Force measurements and slipstream surveys were taken for power coefficients from 0.30 to 1.00 at a free-stream Mach number of 0.40 and for power coefficients from 0.40 to 1.00 at a free-stream Mach number of 0.50. Density altitudes from 20,000 to 45,000 feet were simulated for engine powers from 150 to 2500 brake horsepower, and for engine speeds from 1100 to 2900 rpm.

REDUCTION OF DATA

The method of data reduction was identical to that described in reference 1. The force measurements were analyzed in terms of the variation of the propeller efficiency η with the propeller power coefficient C_P and the advance-diameter ratio J . These quantities were computed from the following equations:

$$C_P = \frac{P}{\rho n^3 D^5}$$

where

D propeller diameter, feet

n propeller rotational speed, revolutions per second

P engine power, foot-pounds per second

ρ free-stream density, slugs per cubic foot

$$J = \frac{V}{nD}$$

where V is the free-stream velocity in feet per second.

$$\eta = \frac{C_T J}{C_P}$$

The propeller thrust coefficient C_T in the efficiency formula was defined as

$$C_T = \frac{T}{\rho n^2 D^4}$$

where T is the propeller thrust in pounds.

Propeller tip Mach number M_t was obtained from the equation

$$M_t = M_o \sqrt{1 + \left(\frac{\pi}{J}\right)^2}$$

where M_o is the free-stream Mach number.

The slipstream surveys are presented as plots of the total-pressure differential $H_s - H_o$ against the square of the radius ratio $(r_s/R)^2$

where

H_o free-stream total pressure, pounds per square foot

H_s total pressure at survey point, pounds per square foot

R propeller radius to tip, inches

r_s radial distance from thrust axis to survey point, inches

RESULTS AND DISCUSSION

The propeller characteristics are presented separately for free-stream Mach numbers of 0.40 and 0.50. Because corrections for tunnel-wall constriction effects on the installation drag and the propeller performance parameters vary with airspeed, data obtained at the two free-stream Mach numbers are not comparable. As in reference 1, the results of the force measurements are of primary value in showing the trends of propeller efficiency for changes in power coefficient and

advance-diameter ratio. Slipstream surveys, which illustrate the blade thrust distribution for several operating conditions, are presented in terms of the difference between the total pressure at the survey point H_s and the free-stream total pressure H_o . (See reference 1.)

Free-stream Mach number, 0.40. - The effect of advance-diameter ratio on propeller efficiency at a free-stream Mach number of 0.40 is presented in figure 4 for a range of power coefficients from 0.30 to 1.00. The variation of propeller efficiency with power coefficient is shown in figure 5 for approximately constant advance-diameter ratios.

Nearly constant peak efficiencies were obtained for power coefficients from 0.30 to 0.70 at advance-diameter ratios from 1.80 to 3.00. (See fig. 4.) As the power coefficient was increased the peak efficiency occurred at progressively higher advance-diameter ratios. An increase in power coefficient from 0.70 to 0.90 reduced the peak efficiency by about 5 percent. (See fig. 4.)

At an advance-diameter ratio of 1.70, the propeller efficiency was reduced about 9 percent for a change in power coefficient from 0.30 to 0.70. (See fig. 5.) An increase in the power coefficient from 0.70 to 0.90 at the same advance-diameter ratio, however, resulted in a 20-percent drop in efficiency. The large drop in efficiency for the high power coefficients in the low range of advance-diameter ratio is attributed to blade tip stall, a result of the excessively high operating angles of attack.

An increase in advance-diameter ratio considerably improved the propeller efficiency at the high power coefficients. For a power coefficient of 0.60, a change in advance-diameter ratio from 1.70 to 2.80 increased the efficiency by about 7 percent, but a similar increase in advance-diameter ratio at a power coefficient of 0.90 resulted in a 25-percent increase in efficiency. (See fig. 5.)

Blade thrust distribution curves corresponding to the test conditions of figure 5 for $J \approx 2.10$ are shown in figure 6. For power coefficients from 0.31 to 0.82, the thrust distribution was uniform and the loading increased steadily with power coefficient. An increase in power coefficient from 0.82 to 0.89 (figs. 6(d) and 6(e)) reduced the over-all thrust loading more than might be expected from the drop in efficiency shown in figure 4 for these conditions. The data for the power coefficient of 0.89 were taken at a higher altitude and a lower engine power than that for the power coefficient of 0.82 and therefore a marked reduction in the thrust loading resulted.

Partial stall at the blade tips, characterized by the drop in total-pressure rise at the outboard blade sections, occurred at a value of C_p of 1.00. (See fig. 6(f).)

The difference between the right and left surveys was apparently due to a misalignment of the thrust axis and the approaching air stream. The right, or downgoing, blades operated at slightly higher angles of attack than the left, or upgoing, blades and consequently were more heavily loaded. (See reference 2.)

Slipstream surveys showing the effect of the advance-diameter ratio on the thrust distribution at a power coefficient of 0.30 are shown in figure 7. The blade thrust load distribution at an advance-diameter ratio of 2.99 (fig. 7(a)) was uniform, with the inboard and outboard sections evenly loaded. As the advance-diameter ratio was reduced to 1.40 (fig. 7(b) to 7(f)), the over-all thrust loading increased; the thrust loading on the outboard sections increased more rapidly than on the inboard sections. Within the range of advance-diameter ratios investigated, at a power coefficient of 0.30, no blade stall was evident. The slight irregularity in the distribution curve at $(r_g/R)^2 = 0.2$ was apparently caused by the propeller shank cuff.

Slipstream surveys are also shown for a power coefficient of 0.90 in figure 8. The blade thrust distribution at an advance-diameter ratio of 3.82 was uniform and similar to that for $C_p = 0.30$ (fig. 7(a)). At an advance-diameter ratio of 2.10, the thrust loading was greater on the outboard blade sections than on the inboard sections. A further decrease in advance-diameter ratio to 1.67 resulted in stalling the blade sections from the blade tip to $(r_g/R)^2 = 0.55$. (See fig. 8(c).) As the outboard sections stall, the required blade angle is increased and consequently the loading on the inboard sections is increased.

Free-stream Mach number, 0.50. - The effect of advance-diameter ratio on propeller efficiency at a free-stream Mach number of 0.50 is presented in figure 9 for a range of power coefficients from 0.40 to 1.00. The variation of propeller efficiency with changes in power coefficient at approximately constant values of advance-diameter ratio is shown in figure 10.

At advance-diameter ratios above 2.90, maximum efficiencies were obtained for power coefficients from 0.80 to 1.00; whereas, at advance-diameter ratios below 2.90, maximum efficiencies were obtained for power coefficients of 0.60 and 0.70. (See fig. 9.) The envelope of the efficiency curves decreased about 12 percent between advance-diameter ratios of 2.60 and 4.20. Changes in the power coefficient from 0.60 to 1.00, within the range of advance-diameter ratios covered, had a

relatively small effect on the propeller efficiency. The spread in efficiency for power coefficients below 0.80 increased at advance-diameter ratios above 3.00. (See fig. 9.)

The effect of increasing power coefficient on blade thrust load distribution is shown in figure 11 for an advance-diameter ratio of approximately 2.90 and in figure 12 for an advance-diameter ratio of 4.20. These surveys correspond to the test conditions shown in figure 10. At an advance-diameter ratio of 2.90, the thrust loading was uniform over the blade and increased steadily as the power coefficient was increased from 0.41 to 0.92 (figs. 11(a) to 11(e)). The survey for $C_p = 1.02$ (fig. 11(f)) indicates a reduction in thrust as compared with the survey for $C_p = 0.92$ (fig. 11(e)), which may be attributed to the slightly higher advance-diameter ratio at which the point was run. As expected, at an advance-diameter ratio of 4.20 for power coefficients from 0.42 to 1.03, the blade thrust loading is relatively low. (See fig. 12.)

The variation of thrust load distribution with changes in advance-diameter ratio for power coefficients of 0.40, 0.70, and 1.00 are shown in figures 13, 14, and 15, respectively. A change in the advance-diameter ratio from 4.20 to 1.75 for a power coefficient of 0.40 resulted in a rapid increase in loading on the outboard sections. For an advance-diameter ratio of 1.75, which corresponds to a tip Mach number of 1.01, the thrust-loading reduction at the tip sections is due to local compressibility effects (fig. 13(e)). A slight drop in propeller efficiency is indicated in figure 9 for the test conditions of figure 13(e). For power coefficients of 0.70 (fig. 14) and 1.00 (fig. 15), the blade thrust distribution was similar, except that the loading on the inboard and outboard sections increased more uniformly, and there was no evidence of blade stall or compressibility effects within the range of advance-diameter ratios investigated.

SUMMARY OF RESULTS

The propeller efficiencies presented in this report are useful primarily in showing the comparative effects of blade loading on propeller performance, because no corrections for tunnel-wall constriction effects on the installation drag and propeller performance parameters have been applied. The investigation in the altitude wind tunnel of the performance at high blade loadings of a Curtiss 839-1C2-1SR1 four-blade propeller on a YP-47M airplane indicated:

1. At a free-stream Mach number of 0.40, nearly constant peak efficiencies were obtained at power coefficients from 0.30 to 0.70. A change in power coefficient from 0.70 to 0.90 reduced the peak efficiency about 5 percent.

2. For an advance-diameter ratio of 1.70 and a free-stream Mach number of 0.40, the propeller efficiency was reduced about 9 percent for a change in power coefficient from 0.30 to 0.70. For power coefficients above 0.70, the efficiency decreased more rapidly.

3. At a free-stream Mach number of 0.50 and advance-diameter ratios above 2.90, the highest propeller efficiencies were obtained for power coefficients from 0.80 to 1.00. At advance-diameter ratios below 2.90, the highest efficiencies were obtained for power coefficients of 0.60 and 0.70. The envelope of the efficiency curves decreased about 12 percent between advance-diameter ratios of 2.60 and 4.20. A change in power coefficient from 0.60 to 1.00, within the range of advance-diameter ratios covered, had a relatively small effect on the propeller efficiency. The spread in efficiency for power coefficients below 0.80 increased at advance-diameter ratios above 3.00.

4. For a free-stream Mach number of 0.40, blade stall at the tip sections, as indicated by slipstream surveys, became evident for a power coefficient of 0.91 when the advance-diameter ratio was reduced to 1.67. At a free-stream Mach number of 0.50, local compressibility effects became evident for a power coefficient of 0.40 when the advance-diameter ratio was decreased to 1.75.

5. In general, the thrust loading on the outboard sections increased more rapidly than on the inboard sections as the power coefficient was increased or as the advance-diameter ratio was decreased.

For conditions where blade stall or compressibility effects were evident the thrust loading on the tip sections decreased and a portion of the load shifted to the inboard sections.

Aircraft Engine Research Laboratory,
National Advisory Committee for Aeronautics,
Cleveland, Ohio.

Lewis E. Wallner
Lewis E. Wallner,
Mechanical Engineer.

Solomon M. Sorin,
Mechanical Engineer.

Approved:

Alfred W. Young,
Mechanical Engineer.

Abe Silverstein,
Aeronautical Engineer.

va

REFERENCES

1. Seari, Martin J., and Wallner, Lewis E.: Altitude-Wind-Tunnel Investigation of Performance of Several Propellers on YP-47M Airplane at High Blade Loading. I - Aeroproducts H20C-162-X11M2 Four-Blade Propeller. NACA RM No. E6I24, Army Air Forces, 1946.
2. Pondley, Robert E.: Effect of Propeller-Axis Angle of Attack on Thrust Distribution over the Propeller Disk in Relation to Wake-Survey Measurement of Thrust. NACA ACR No. L5J02b, 1945.

INDEX OF FIGURES

	Page
Figure 1. - Blade-form curves for Curtiss 838-1C2-18R1 four-blade propeller. b , section chord; D , propeller diameter; h , section thickness; R , radius to tip; r , section radius.	F-1
Figure 2. - Curtiss 838-1C2-18R1 propeller blade.	F-2
Figure 3. - Front view of YP-47M airplanes with Curtiss 838-1C2-18R1 four-blade propeller installed in altitude-wind-tunnel test section.	F-3
Figure 4. - Characteristics of Curtiss 838-1C2-18R1 four-blade propeller on YP-47M airplane at free-stream Mach number M_0 of approximately 0.40.	F-4
Figure 5. - Effect of power coefficient C_p on propeller efficiency η at constant advance-diameter ratios at free-stream Mach number M_0 of approximately 0.40. Curtiss 838-1C2-18R1 four-blade propeller.	F-5
Figure 6. - Effect of power coefficient C_p on blade thrust load distribution at advance-diameter ratio J of approximately 2.10 and free-stream Mach number M_0 of approximately 0.40. Curtiss 838-1C2-18R1 four-blade propeller.	
(a) C_p , 0.31; J , 1.98; M_0 , 0.39; M_t , 0.74	F-6
(b) C_p , 0.61; J , 2.16; M_0 , 0.40; M_t , 0.70	F-6
(c) C_p , 0.71; J , 2.10; M_0 , 0.39; M_t , 0.70	F-7
(d) C_p , 0.82; J , 2.12; M_0 , 0.39; M_t , 0.70	F-7
(e) C_p , 0.89; J , 2.10; M_0 , 0.39; M_t , 0.70	F-8
(f) C_p , 1.00; J , 2.05; M_0 , 0.38; M_t , 0.70	F-8
Figure 7. - Effect of advance-diameter ratio J on blade thrust load distribution at power coefficient C_p of approximately 0.30 and free-stream Mach number M_0 of approximately 0.40. Curtiss 838-1C2-18R1 four-blade propeller.	
(a) C_p , 0.29; J , 2.99; M_0 , 0.40; M_t , 0.58	F-9
(b) C_p , 0.30; J , 2.30; M_0 , 0.39; M_t , 0.66	F-9
(c) C_p , 0.31; J , 1.98; M_0 , 0.39; M_t , 0.74	F-10
(d) C_p , 0.30; J , 1.90; M_0 , 0.39; M_t , 0.78	F-10
(e) C_p , 0.30; J , 1.70; M_0 , 0.40; M_t , 0.84	F-11
(f) C_p , 0.30; J , 1.40; M_0 , 0.39; M_t , 0.97	F-11

Page

Figure 8. - Effect of advance-diameter ratio J on blade thrust load distribution at power coefficient C_p of approximately 0.90 and free-stream Mach number M_o of approximately 0.40. Curtiss 838-1C2-18R1 four-blade propeller.

(a) C_p , 0.89; J , 3.82; M_o , 0.40; M_t , 0.51	F-12
(b) C_p , 0.89; J , 2.10; M_o , 0.39; M_t , 0.70	F-12
(c) C_p , 0.91; J , 1.67; M_o , 0.38; M_t , 0.81	F-12

Figure 9. - Characteristics of Curtiss 838-1C2-18R1 four-blade propeller on YP-47M airplane at free-stream Mach number M_o of approximately 0.50. F-13

Figure 10. - Effect of power coefficient C_p on propeller efficiency η at free-stream Mach number M_o of approximately 0.50. Curtiss 838-1C2-18R1 four-blade propeller. . F-14

Figure 11. - Effect of power coefficient C_p on blade thrust load distribution at advance-diameter ratio J of approximately 2.80 and free-stream Mach number M_o of approximately 0.50. Curtiss 838-1C2-18R1 four-blade propeller. .

(a) C_p , 0.41; J , 2.75; M_o , 0.49; M_t , 0.75	F-15
(b) C_p , 0.60; J , 2.73; M_o , 0.49; M_t , 0.75	F-15
(c) C_p , 0.72; J , 2.92; M_o , 0.50; M_t , 0.73	F-16
(d) C_p , 0.83; J , 2.94; M_o , 0.50; M_t , 0.73	F-16
(e) C_p , 0.92; J , 2.90; M_o , 0.50; M_t , 0.74	F-17
(f) C_p , 1.02; J , 3.02; M_o , 0.50; M_t , 0.72	F-17

Figure 12. - Effect of power coefficient C_p on propeller efficiency η at advance-diameter ratio J of approximately 4.20 and free-stream Mach number M_o of approximately 0.50. Curtiss 838-1C2-18R1 four-blade propeller.

(a) C_p , 0.42; J , 4.20; M_o , 0.49; M_t , 0.62	F-18
(b) C_p , 0.71; J , 4.21; M_o , 0.49; M_t , 0.62	F-18
(c) C_p , 0.82; J , 4.23; M_o , 0.49; M_t , 0.61	F-18
(d) C_p , 0.94; J , 4.23; M_o , 0.49; M_t , 0.61	F-19
(e) C_p , 1.03; J , 4.23; M_o , 0.49; M_t , 0.62	F-19

Page

Figure 13. - Effect of advance-diameter ratio J on blade thrust load distribution at power coefficient C_p of approximately 0.40 and free-stream Mach number M_o of approximately 0.50. Curtiss 838-1C2-18R1 four-blade propeller.

(a)	C_p , 0.42;	J , 4.20;	M_o , 0.49;	M_t , 0.62	F-20
(b)	C_p , 0.41;	J , 3.42;	M_o , 0.50;	M_t , 0.68	F-20
(c)	C_p , 0.41;	J , 2.75;	M_o , 0.49;	M_t , 0.75	F-20
(d)	C_p , 0.41;	J , 2.20;	M_o , 0.49;	M_t , 0.86	F-21
(e)	C_p , 0.41;	J , 1.75;	M_o , 0.49;	M_t , 1.01	F-21

Figure 14. - Effect of advance-diameter ratio J on blade thrust load distribution at power coefficient C_p of approximately 0.70 and free-stream Mach number M_o of approximately 0.50. Curtiss 838-1C2-18R1 four-blade propeller.

(a)	C_p , 0.71;	J , 4.21;	M_o , 0.49;	M_t , 0.61	F-22
(b)	C_p , 0.72;	J , 3.43;	M_o , 0.50;	M_t , 0.68	F-22
(c)	C_p , 0.72;	J , 2.92;	M_o , 0.50;	M_t , 0.73	F-22
(d)	C_p , 0.71;	J , 2.59;	M_o , 0.50;	M_t , 0.79	F-23
(e)	C_p , 0.71;	J , 2.38;	M_o , 0.50;	M_t , 0.82	F-23

Figure 15. - Effect of advance-diameter ratio J on blade thrust load distribution at power coefficient C_p of approximately 1.00 and free-stream Mach number M_o of approximately 0.50. Curtiss 838-1C2-18R1 four-blade propeller.

(a)	C_p , 1.03;	J , 4.23;	M_o , 0.49;	M_t , 0.62	F-24
(b)	C_p , 1.03;	J , 3.67;	M_o , 0.50;	M_t , 0.65	F-24
(c)	C_p , 1.02;	J , 3.41;	M_o , 0.50;	M_t , 0.68	F-25
(d)	C_p , 1.02;	J , 3.02;	M_o , 0.50;	M_t , 0.72	F-25

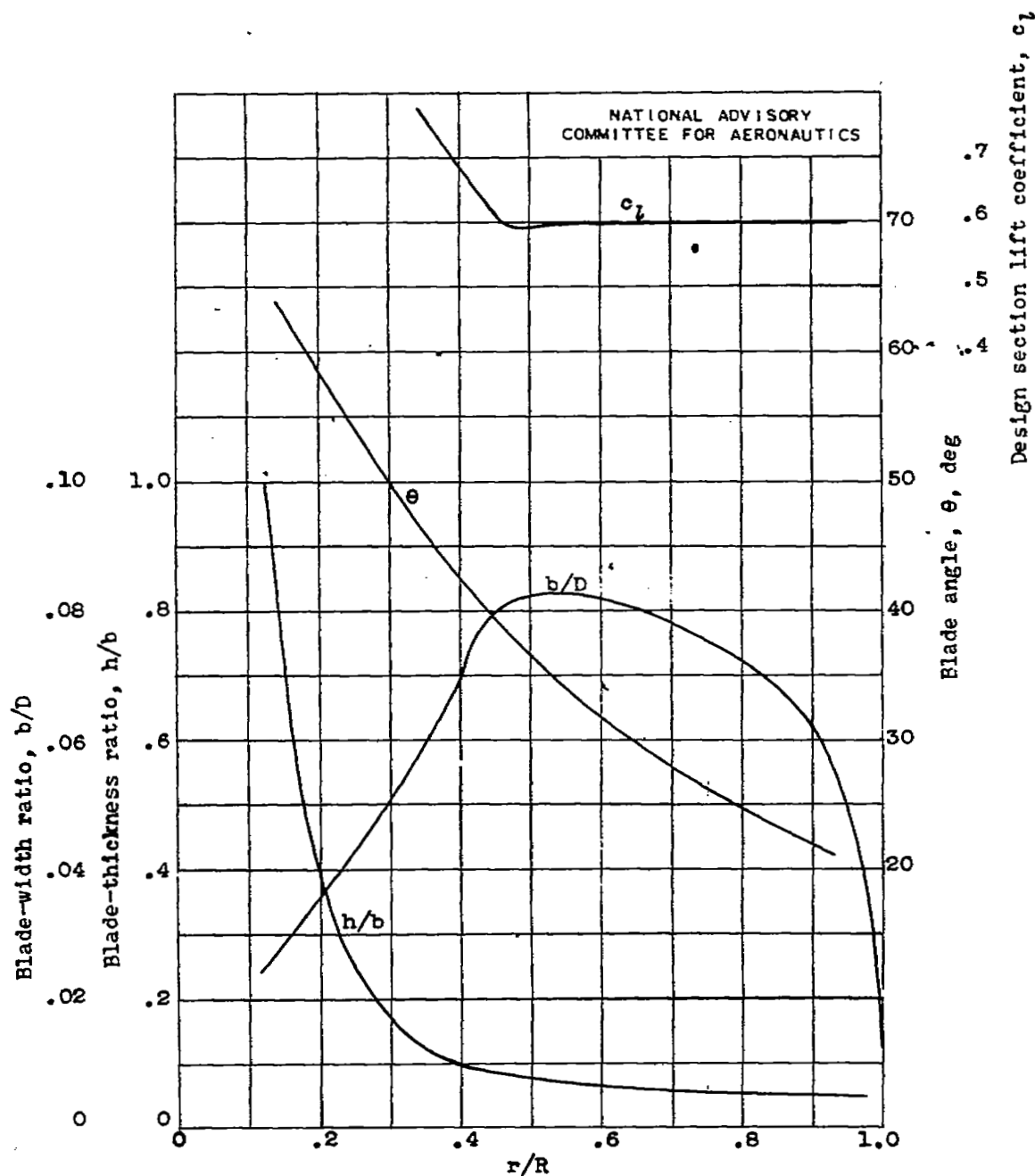


Figure 1.- Blade-form curves for Curtiss 838-1C2-18R1 four-blade propeller. b , section chord; D , propeller diameter; h , section thickness; R , radius to tip; r , section radius.

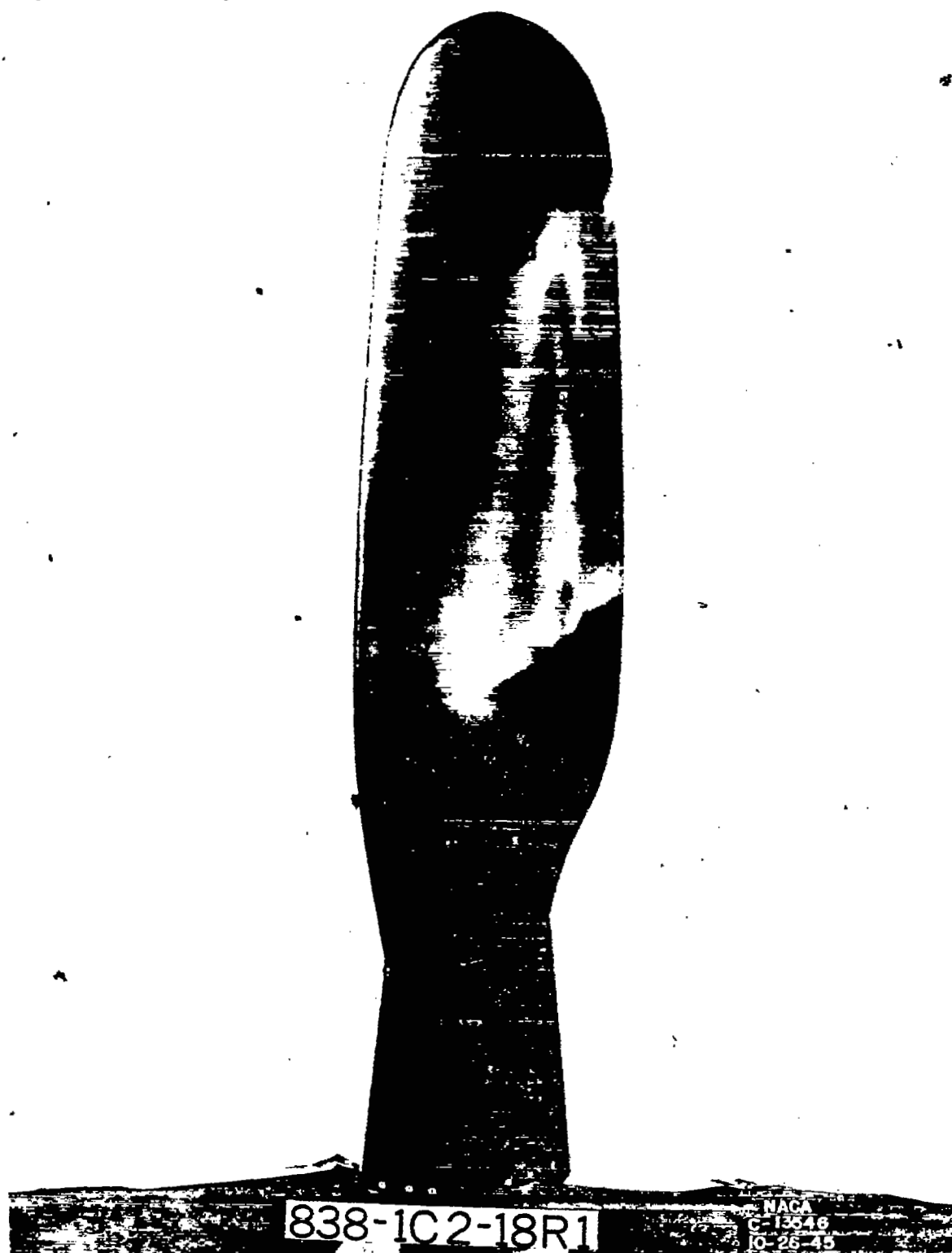


Figure 2. - Curtiss 838-1C2-18R1 propeller blade.

65

NACA RM No. E6J14

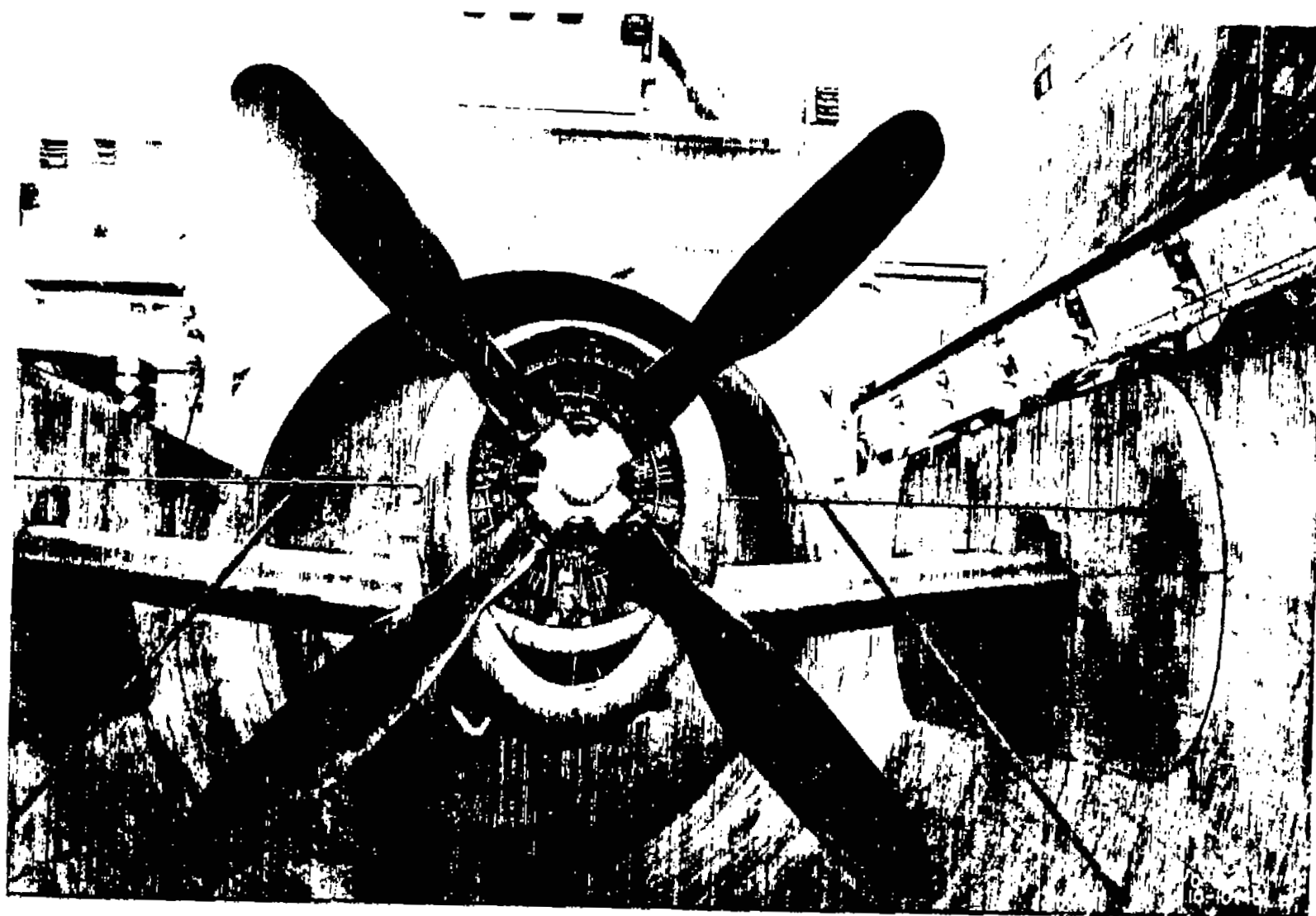


Figure 3. - Front view of YP-47M airplane with Curtiss 838-112-18R1 four-blade propeller installed in altitude-wind-tunnel test section.

4-3

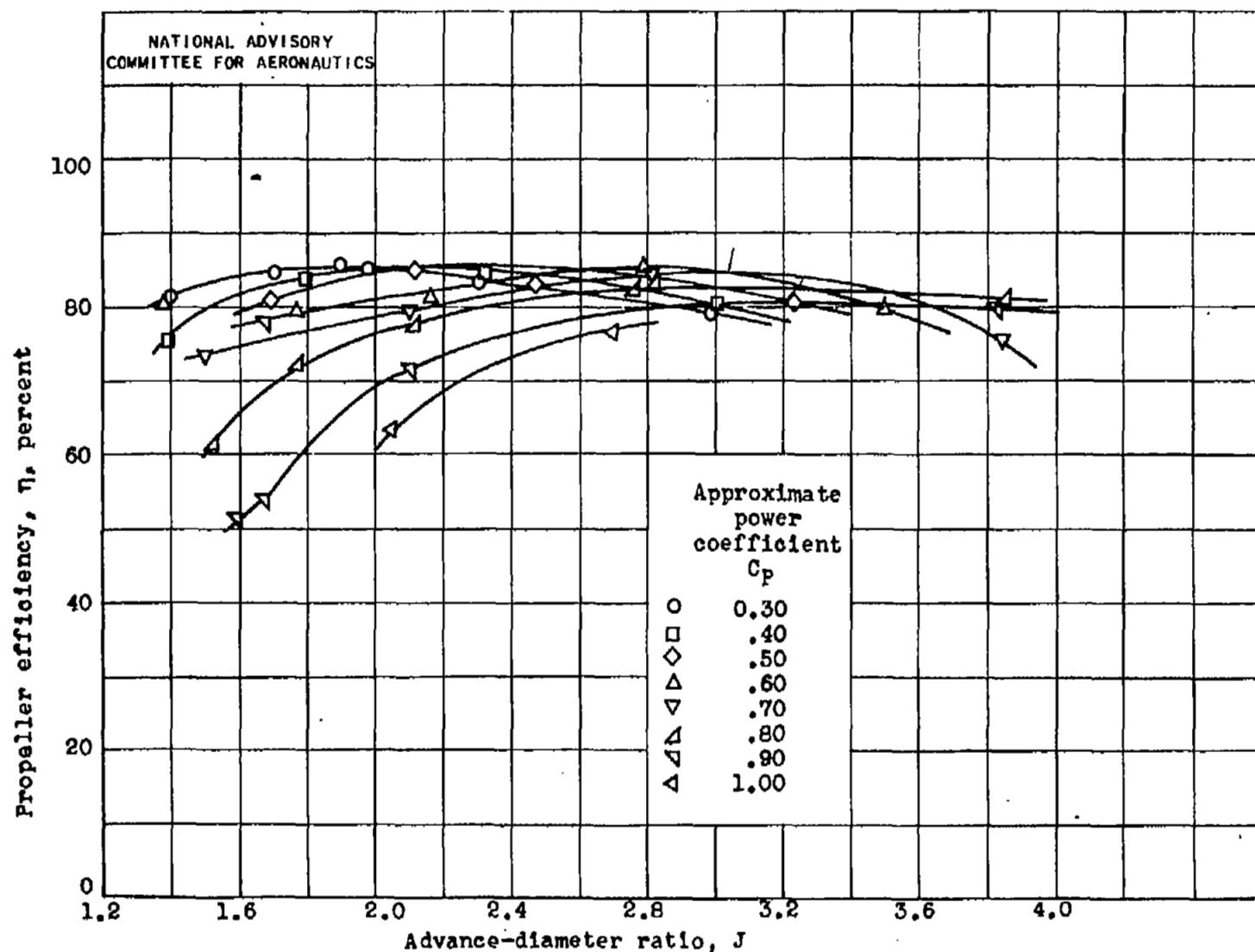


Figure 4.- Characteristics of Curtiss 838-1C2-18R1 four-blade propeller on YP-47M airplane at free-stream Mach number M_0 of approximately 0.40.

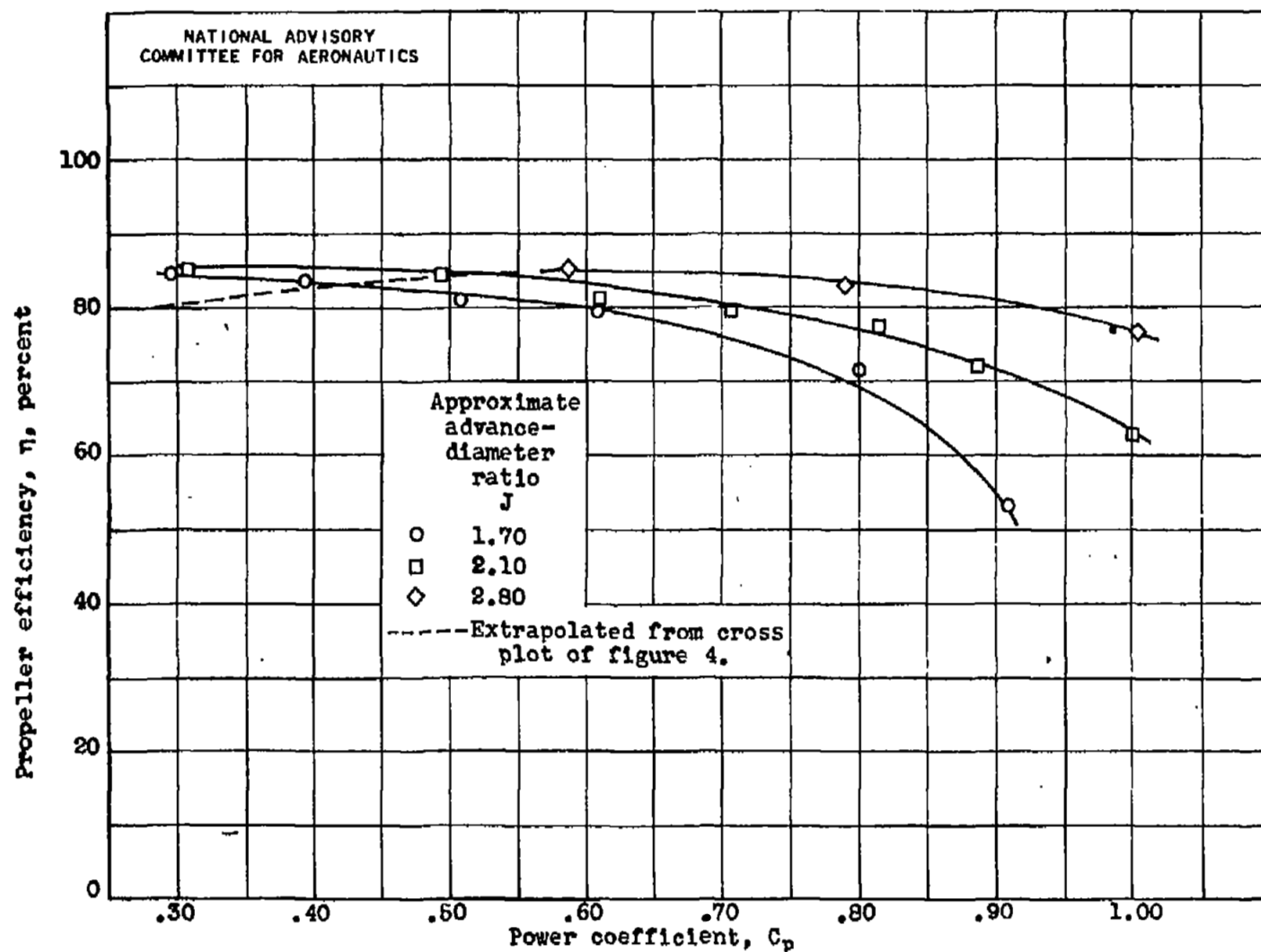


Figure 5.- Effect of power coefficient C_p on propeller efficiency η at constant advance-diameter ratios at free-stream Mach number M_0 of approximately 0.40. Curtiss 838-1C2-18R1 four-blade propeller.

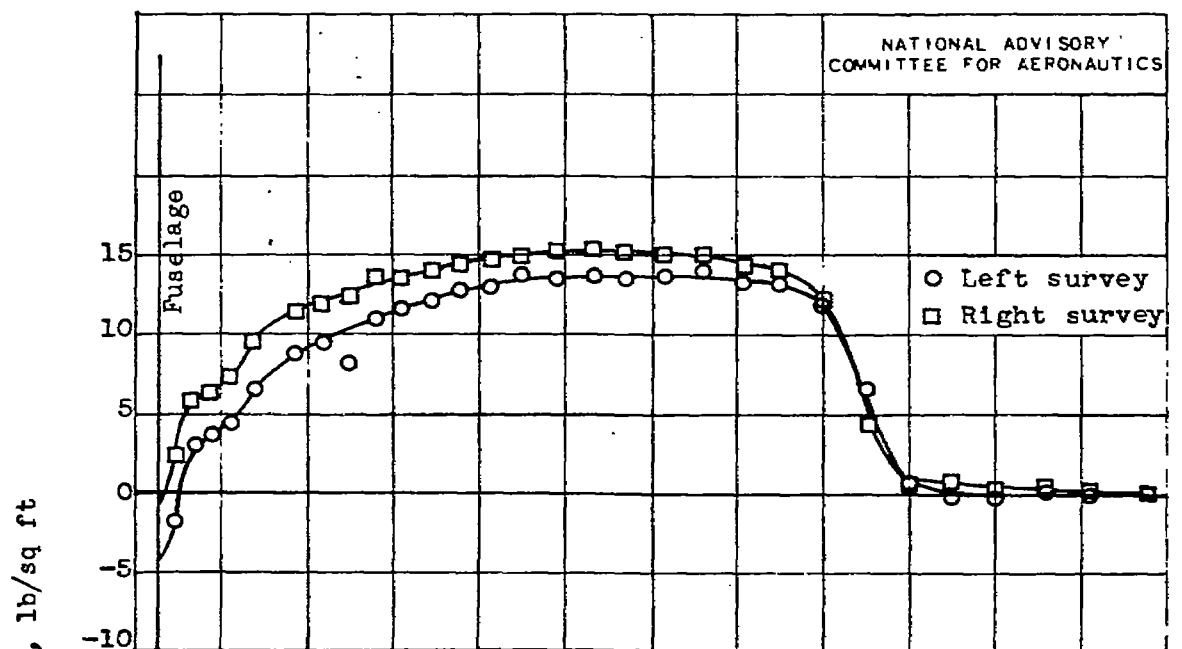
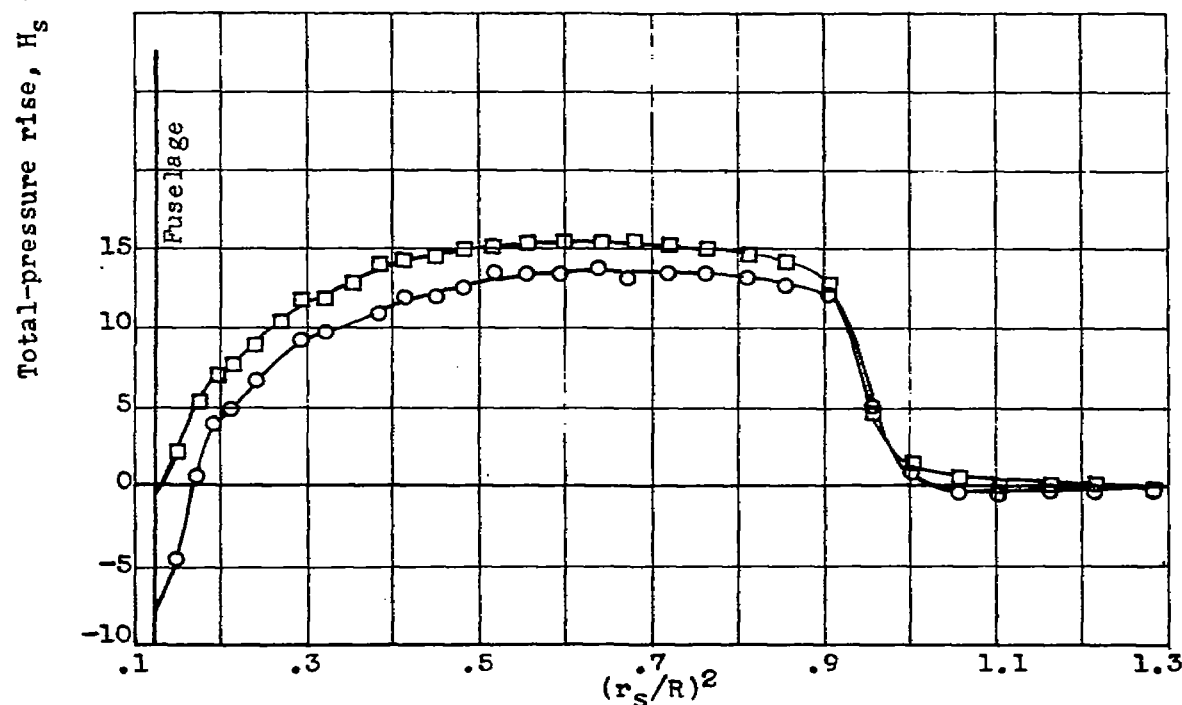
(a) C_p , 0.31; J , 1.98; M_o , 0.39; M_t , 0.74.(b) C_p , 0.61; J , 2.16; M_o , 0.40; M_t , 0.70.

Figure 6.- Effect of power coefficient C_p on blade thrust load distribution at advance-diameter ratio J of approximately 2.10 and free-stream Mach number M_o of approximately 0.40. Curtiss 838-1C2-18R1 four-blade propeller.

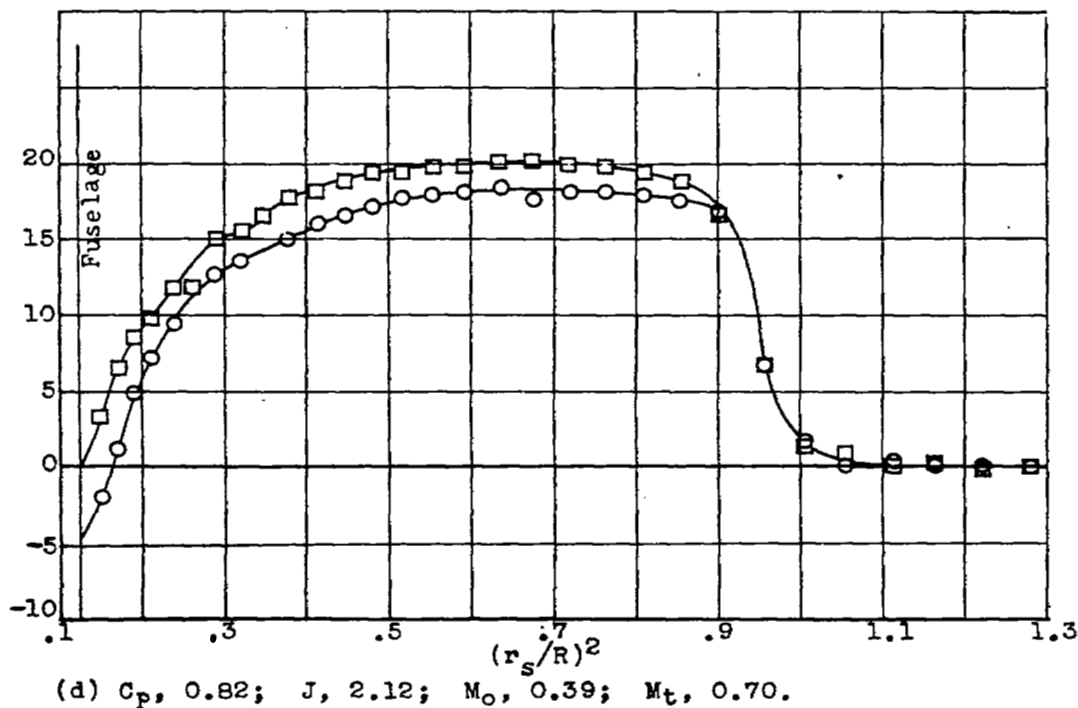
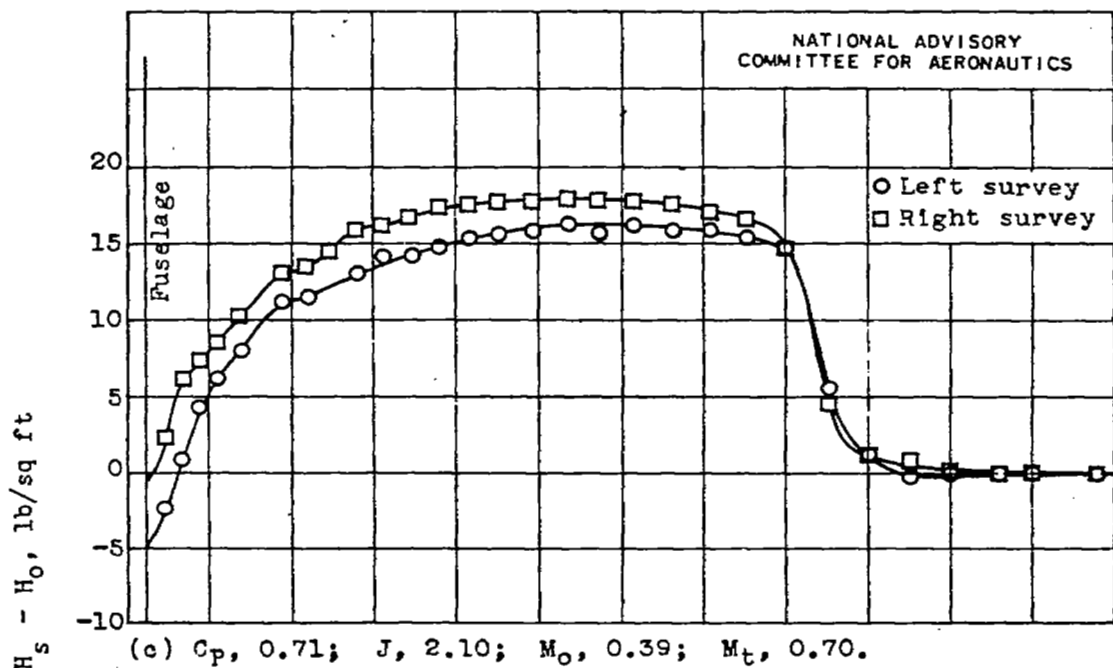


Figure 6.- Continued. Effect of power coefficient C_p on blade thrust load distribution at advance-diameter ratio J of approximately 2.10 and free-stream Mach number M_0 of approximately 0.40. Curtiss 838-1C2-18R1 four-blade propeller.

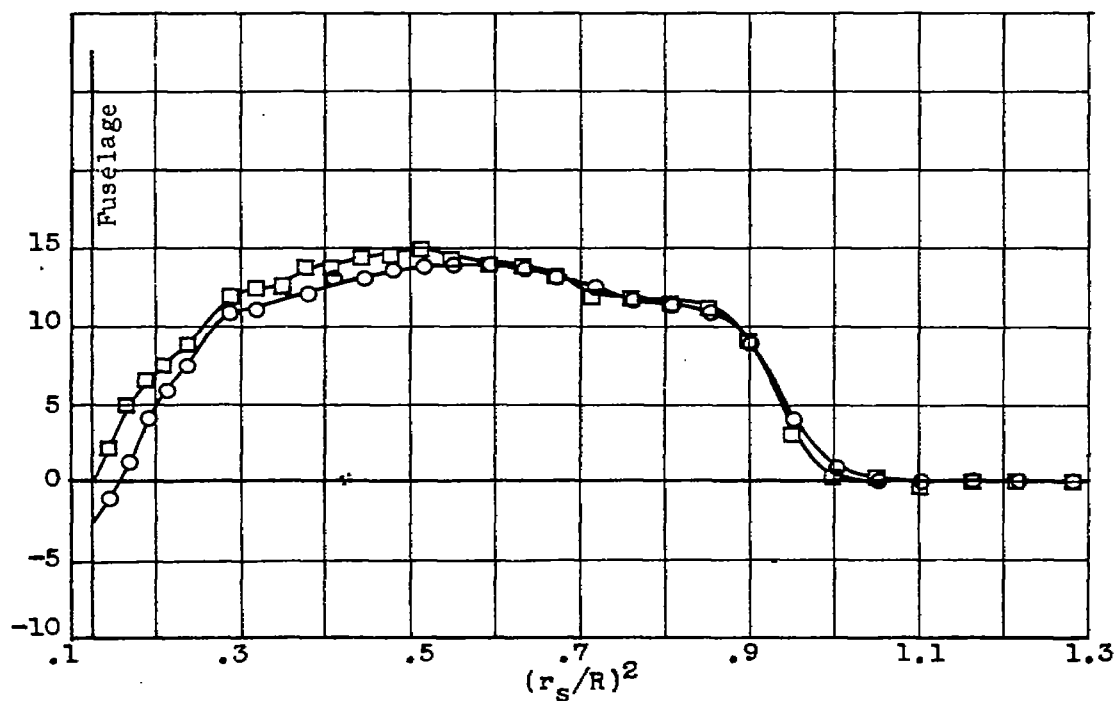
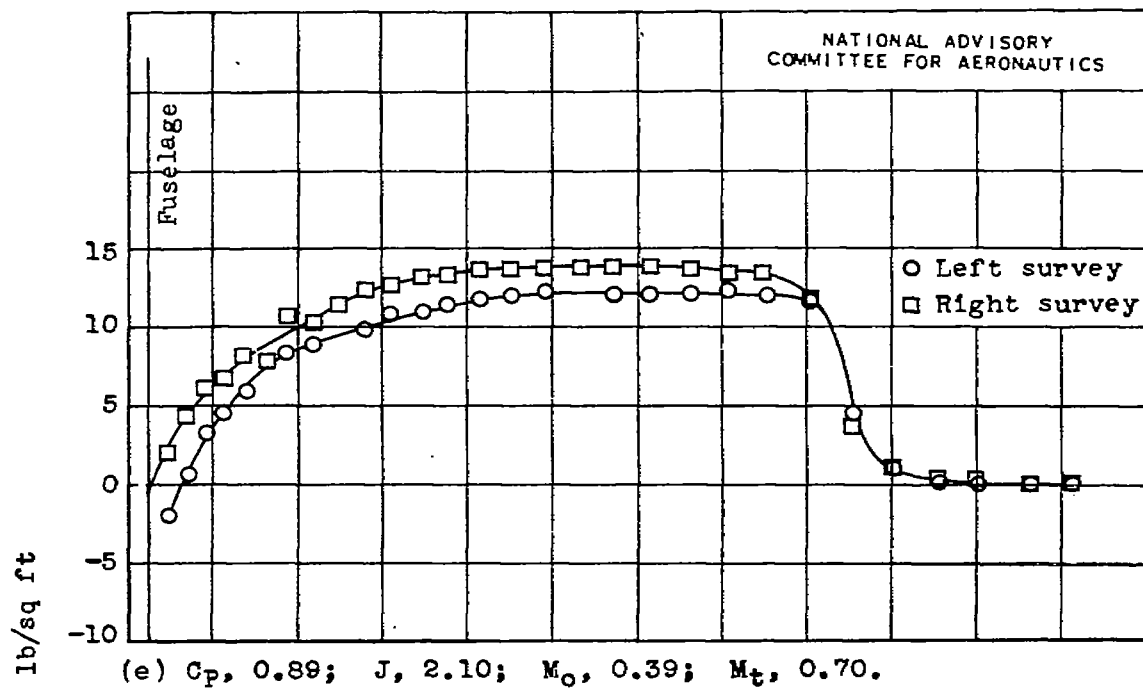


Figure 6.- Concluded. Effect of power coefficient C_p on blade thrust load distribution at advance-diameter ratio J of approximately 2.10 and free-stream Mach number M_o of approximately 0.40. Curtiss 838-102-18R1 four-blade propeller.

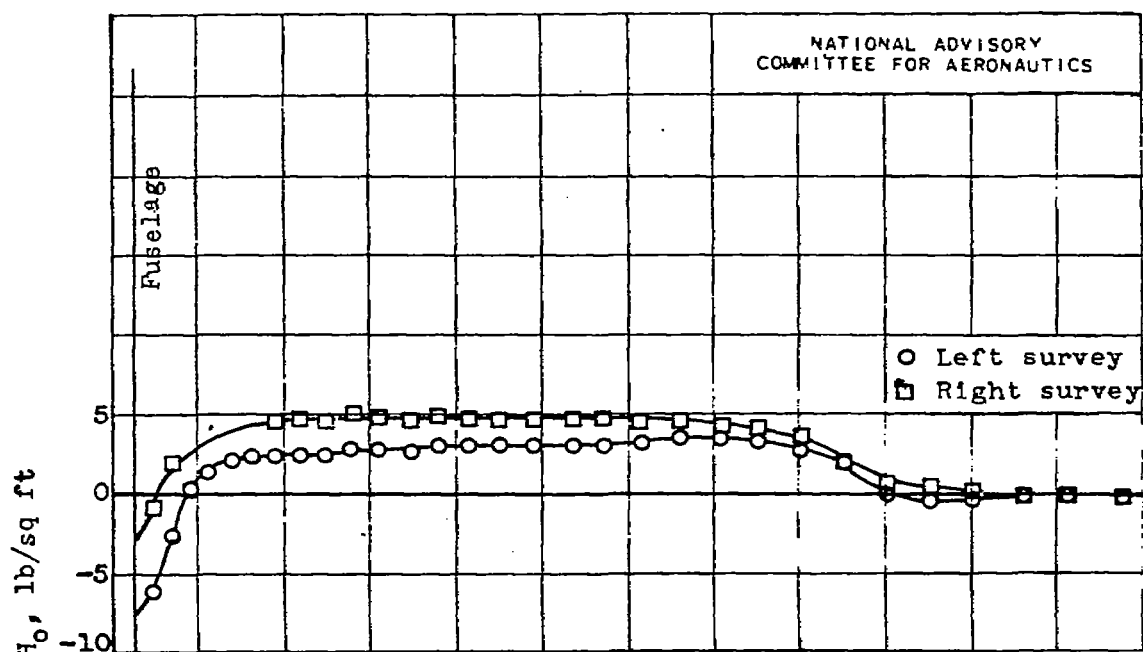
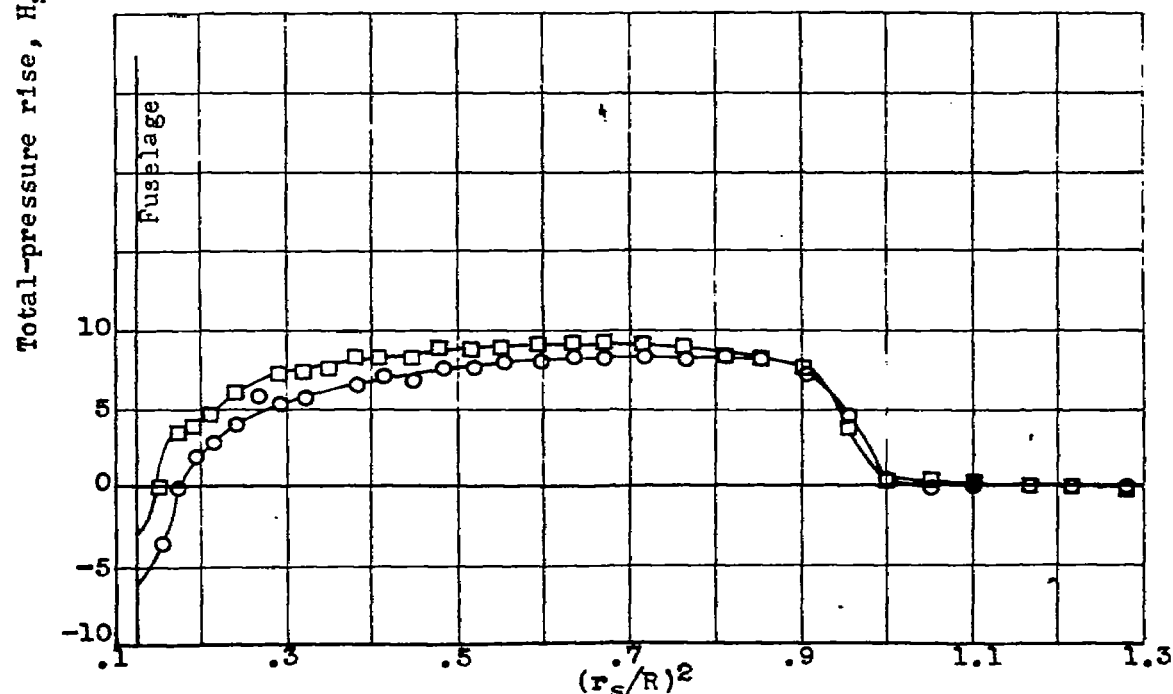
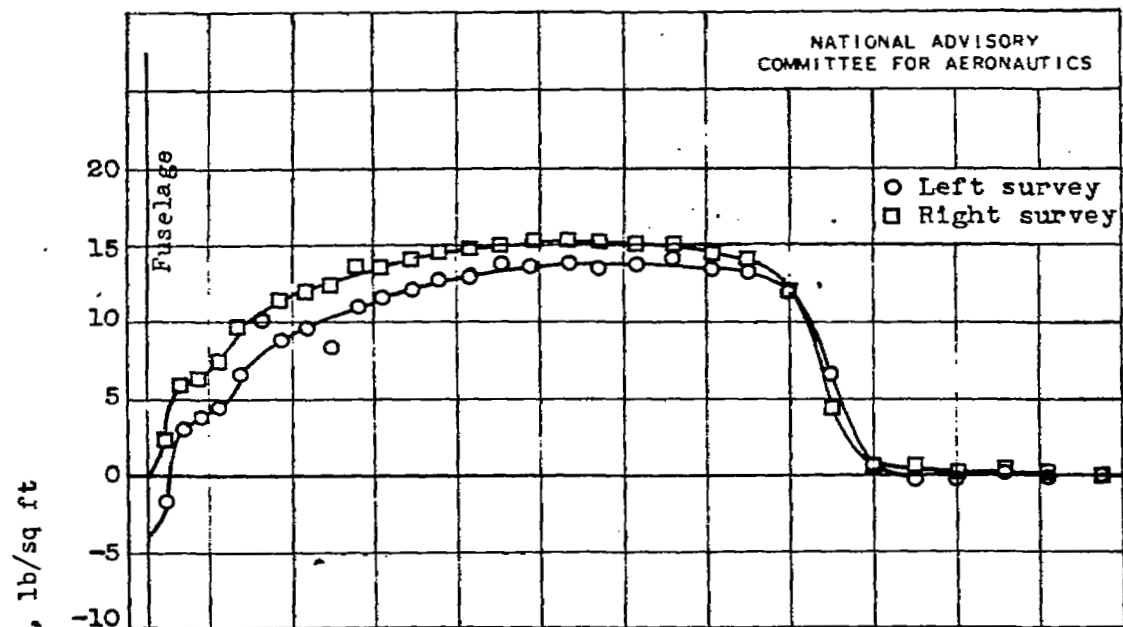
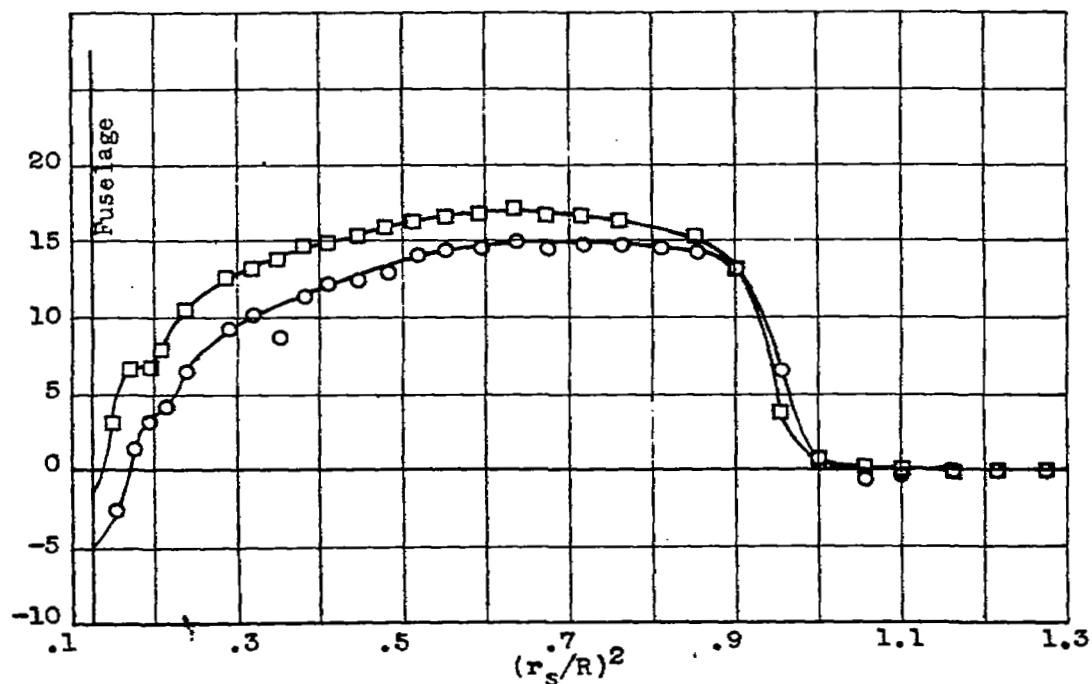
(a) C_p , 0.29; J , 2.99; M_o , 0.40; M_t , 0.58.(b) C_p , 0.30; J , 2.30; M_o , 0.39; M_t , 0.66.

Figure 7.- Effect of advance-diameter ratio J on blade thrust load distribution at power coefficient C_p of approximately 0.30 and free-stream Mach number M_o of approximately 0.40. Curtiss 838-1C2-18R1 four-blade propeller.



(c) C_p , 0.31; J , 1.98; M_o , 0.39; M_t , 0.74.



(d) C_p , 0.30; J , 1.90; M_o , 0.39; M_t , 0.76.

Figure 7.- Continued. Effect of advance-diameter ratio J on blade thrust load distribution at power coefficient C_p of approximately 0.30 and free-stream Mach number M_o of approximately 0.40. Curtiss 838-1C2-18R1 four-blade propeller.

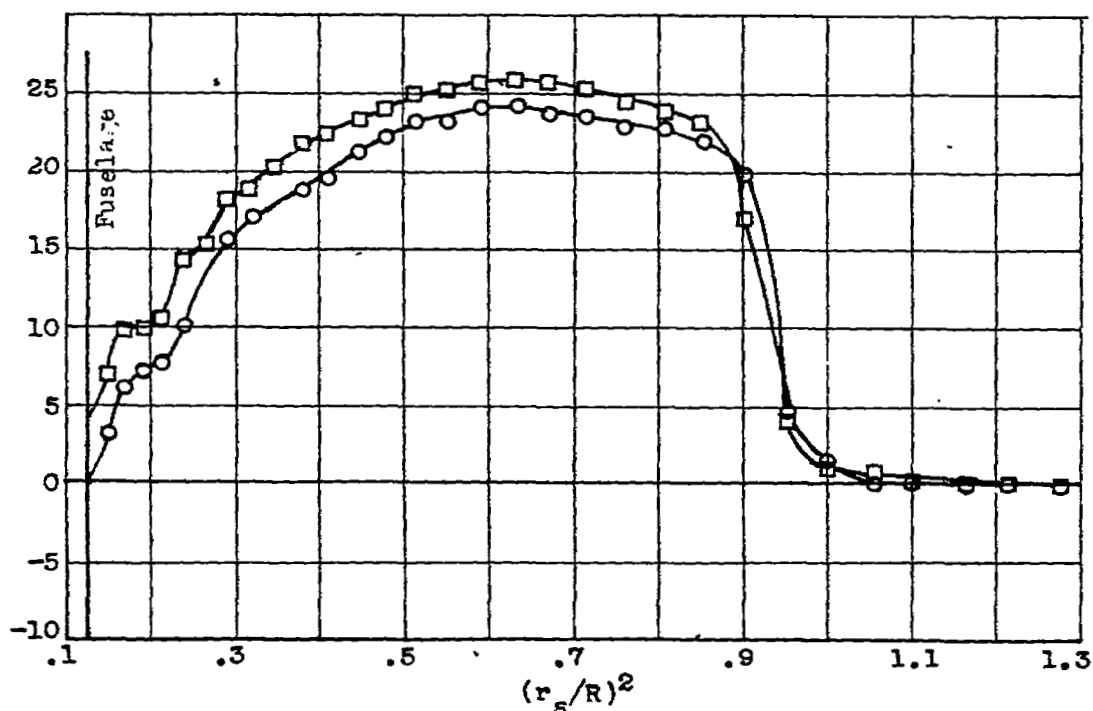
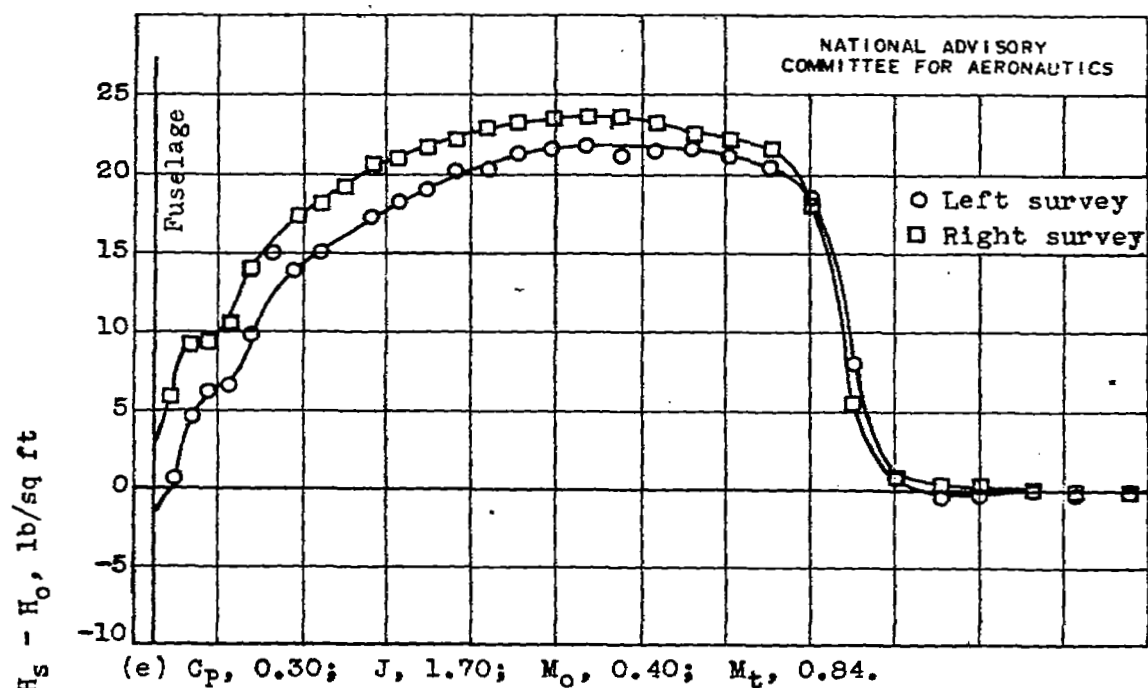


Figure 7.- Concluded. Effect of advance-diameter ratio J on blade thrust load distribution at power coefficient C_p of approximately 0.30 and free-stream Mach number M_o of approximately 0.40. Curtiss 838-1C2-18R1 four-blade propeller.

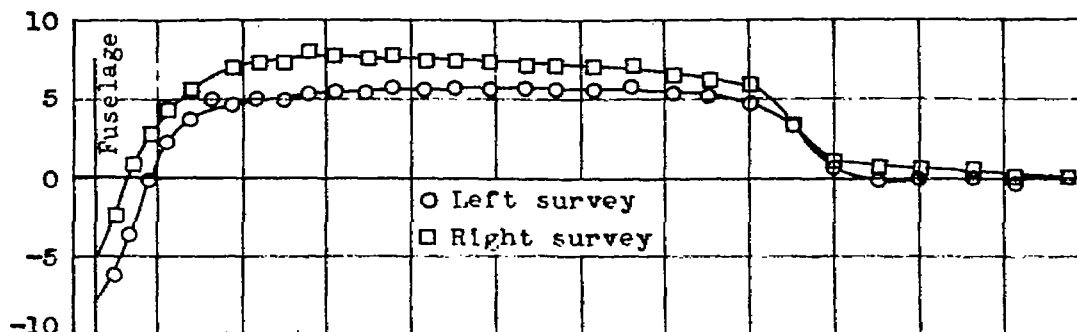
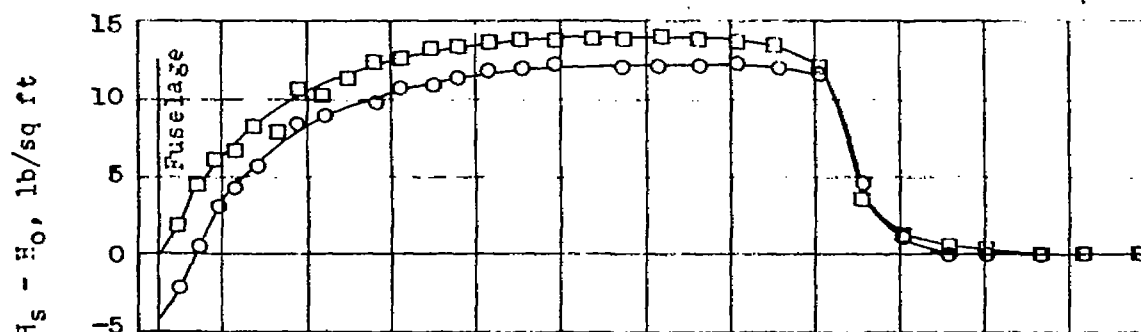
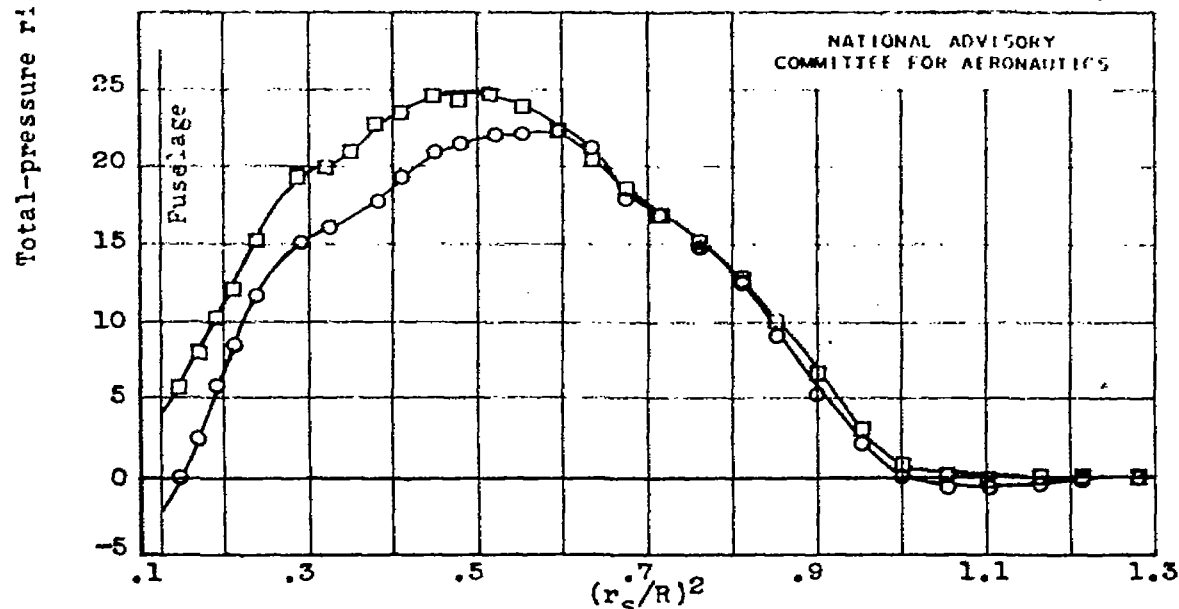
(a) C_p , 0.89; J , 3.82; M_o , 0.40; M_t , 0.51.(b) C_p , 0.89; J , 2.10; M_o , 0.39; M_t , 0.70.(c) C_p , 0.91; J , 1.67; M_o , 0.38; M_t , 0.81.

Figure 8.- Effect of advance-diameter ratio J on blade thrust load distribution at power coefficient C_p of approximately 0.90 and free-stream Mach number M_o of approximately 0.40. Curtiss 838-1C2-18R1 four-blade propeller.

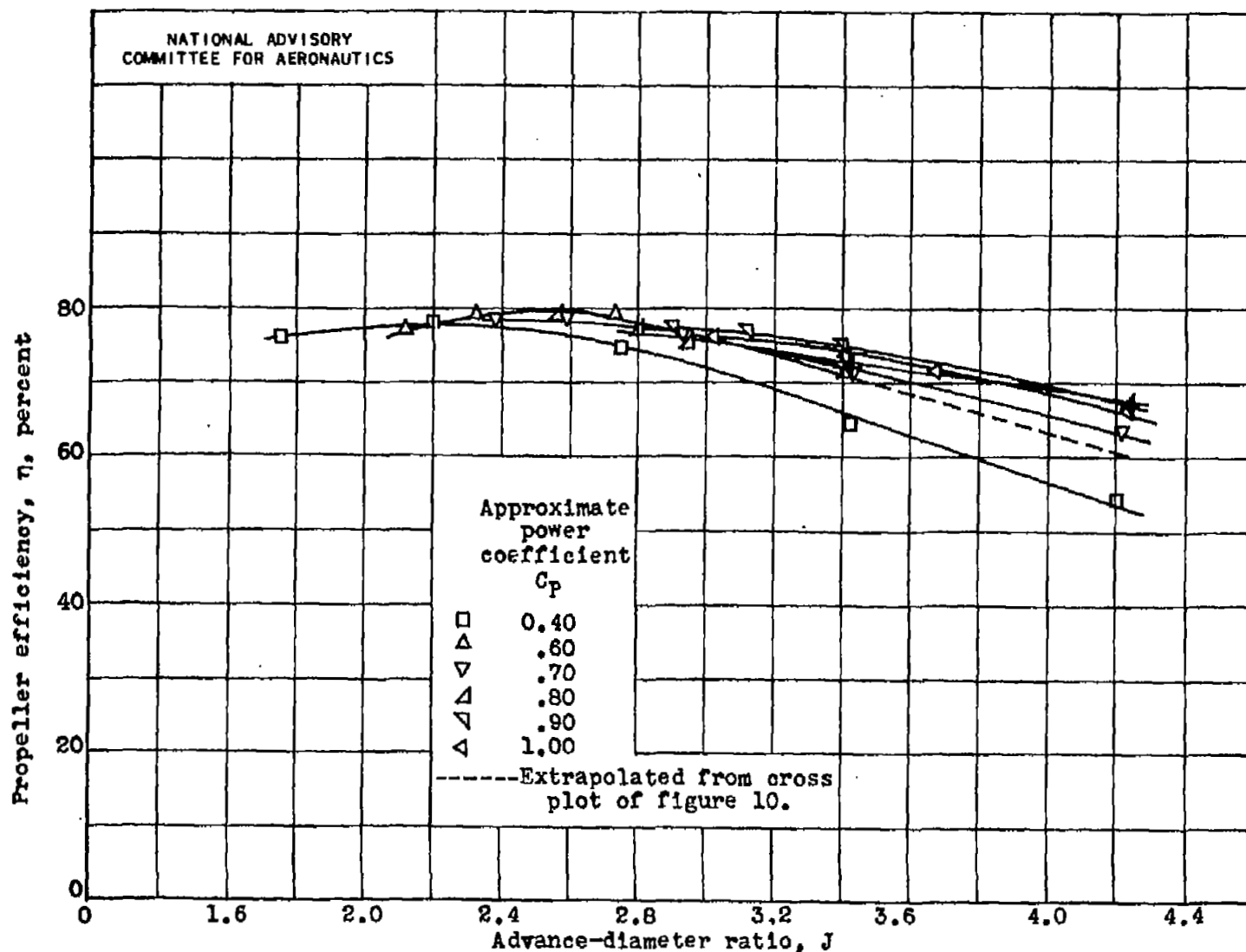


Figure 9.- Characteristics of Curtiss 838-1C2-18R1 four-blade propeller on YP-47M airplane at free-stream Mach number M_0 of approximately 0.50.

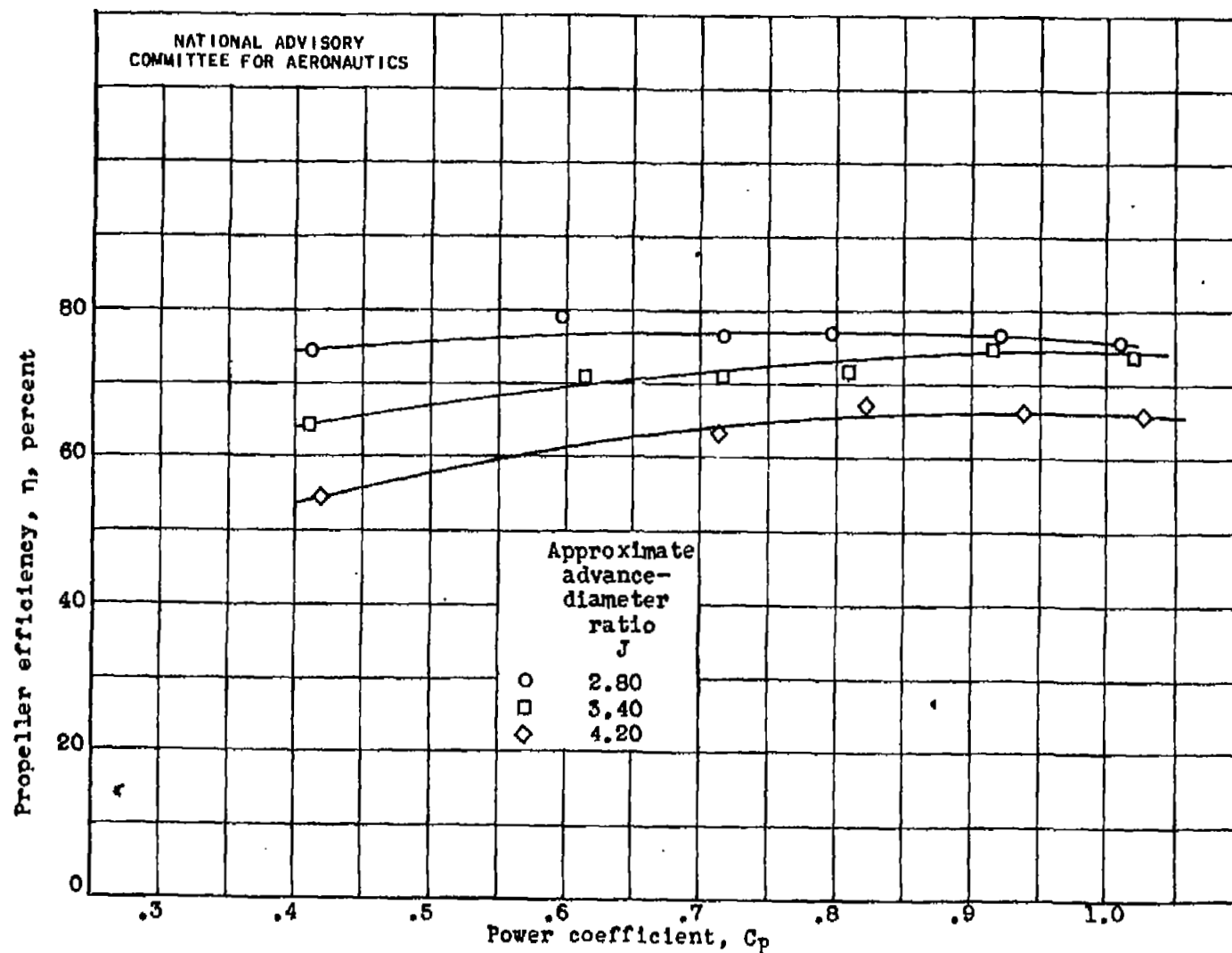
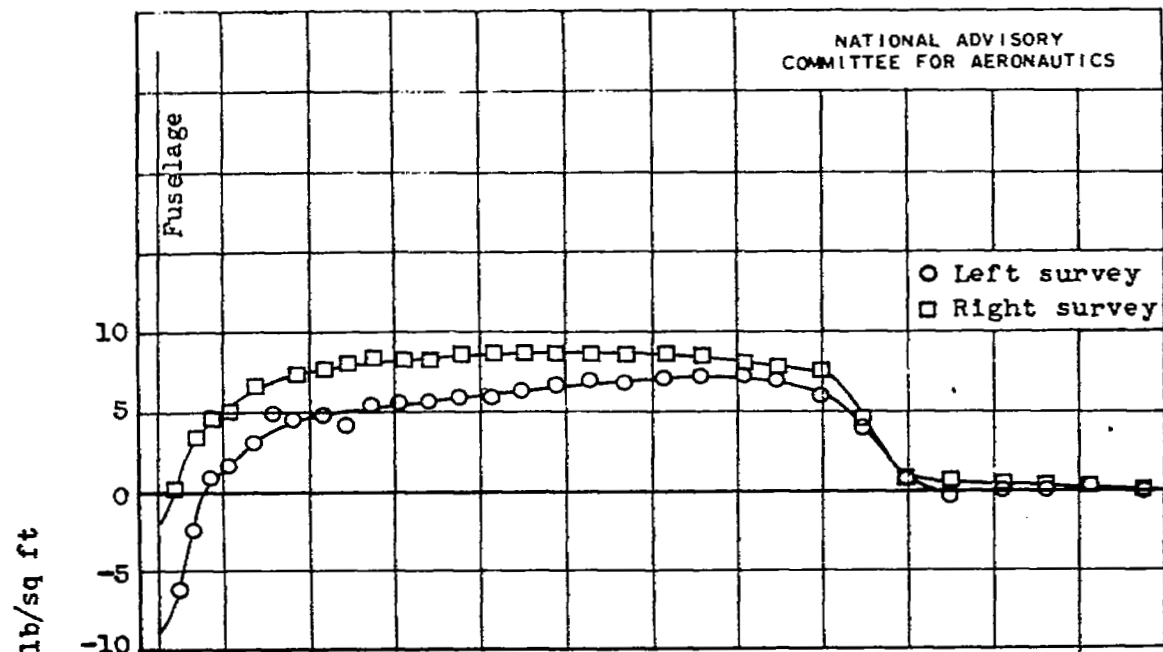
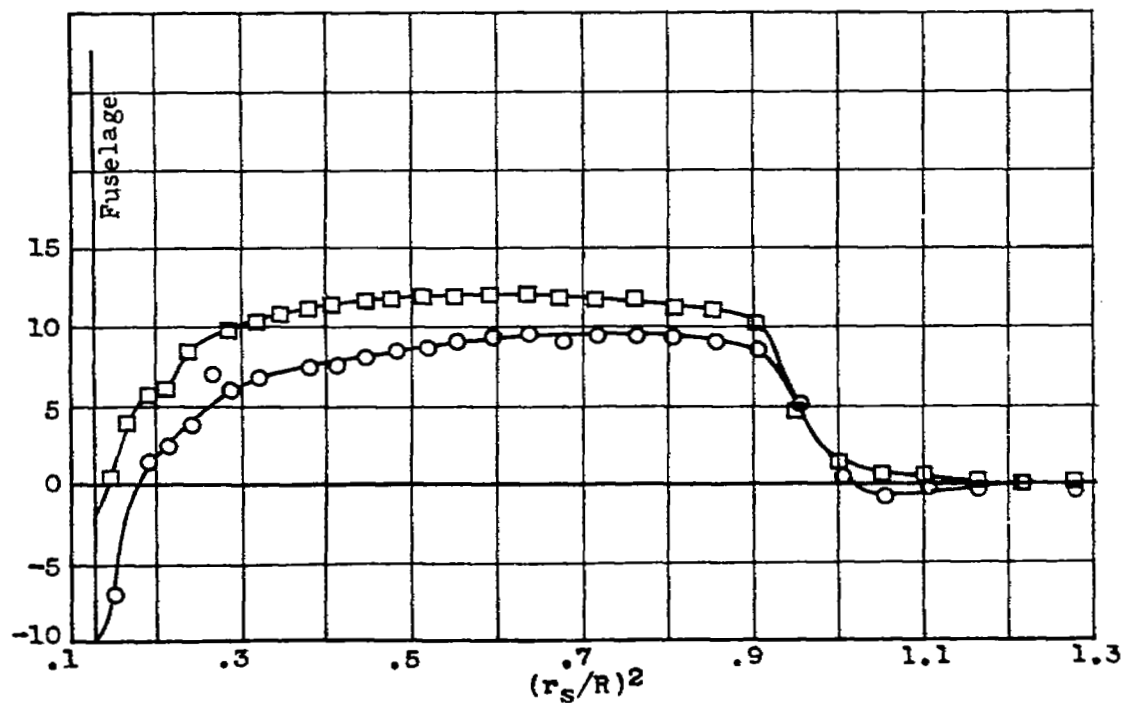


Figure 10.- Effect of power coefficient C_p on propeller efficiency η at free-stream Mach number M_o of approximately 0.50. Curtiss 838-LC2-18R1 four-blade propeller.



(a) C_p , 0.41; J , 2.75; M_o , 0.49; M_t , 0.75.



(b) C_p , 0.60; J , 2.73; M_o , 0.49; M_t , 0.75.

Figure 11.- Effect of power coefficient C_p on blade thrust load distribution at advance-diameter ratio J of approximately 2.90 and free-stream Mach number M_o of approximately 0.50. Curtiss 838-1C2-18R1 four-blade propeller.

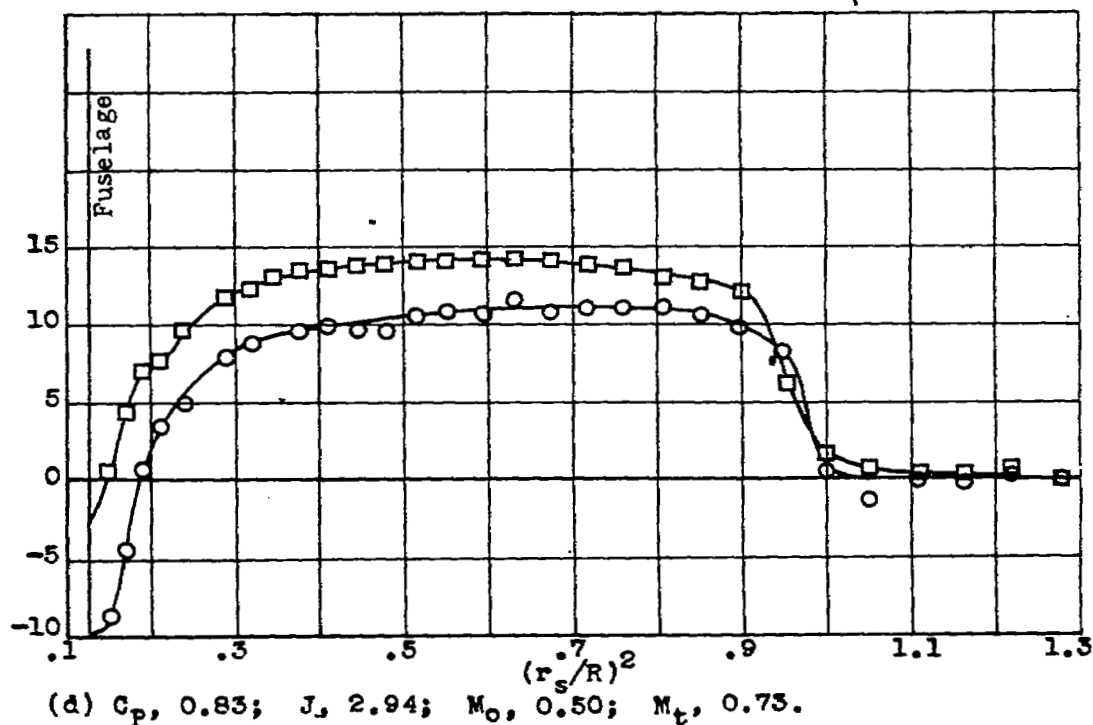
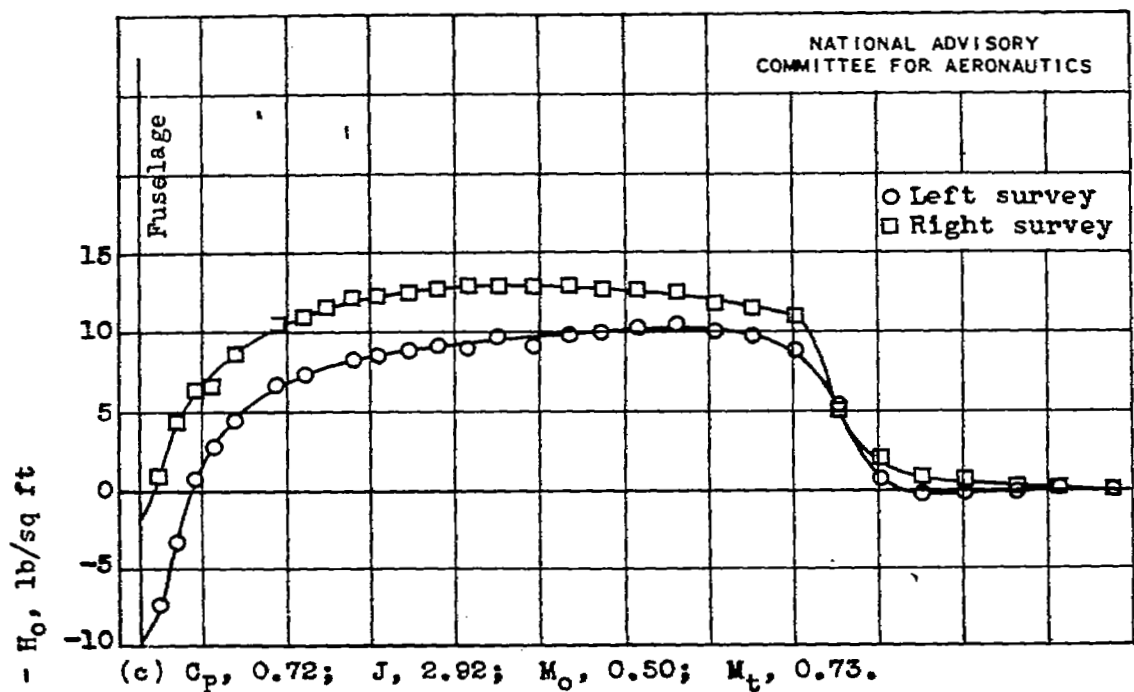


Figure 11.- Continued. Effect of power coefficient C_p on blade thrust load distribution at advance-diameter ratio J of approximately 2.90 and free-stream Mach number M_0 of approximately 0.50. Curtiss 838-1C2-18R1 four-blade propeller.

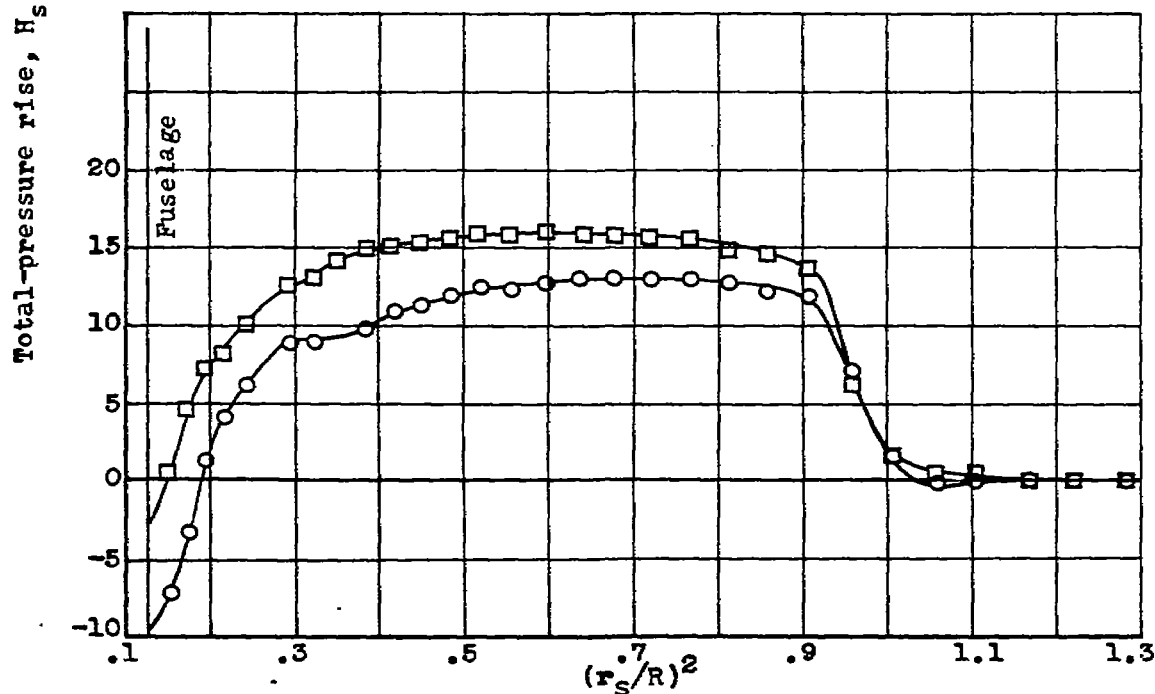
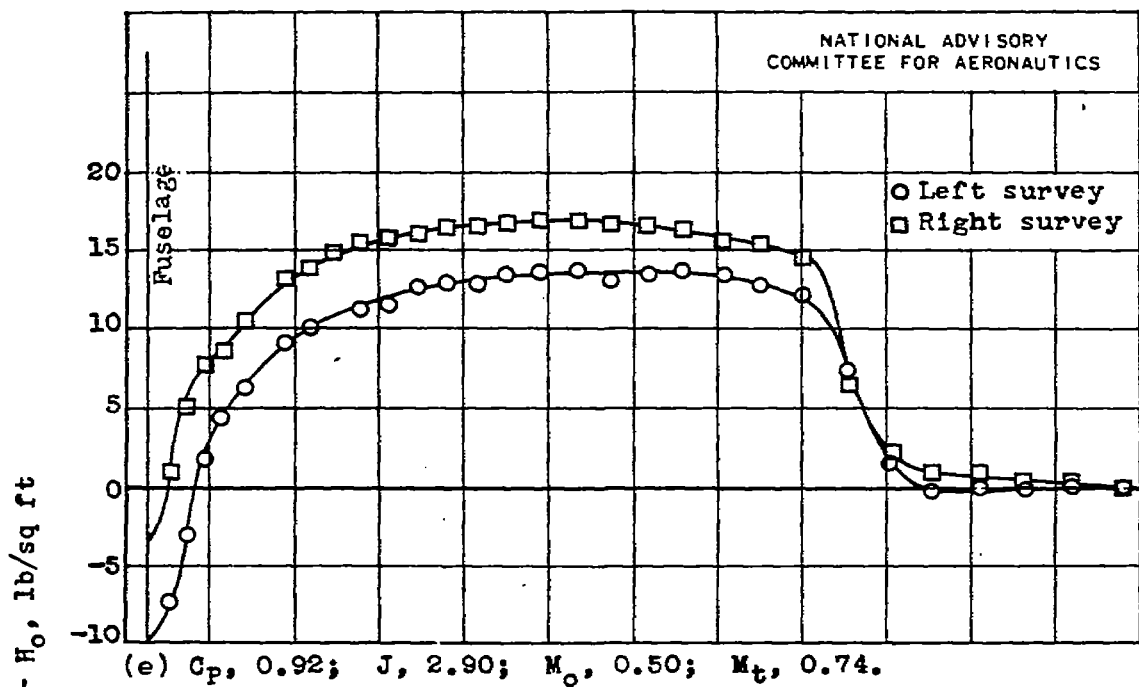


Figure 11.- Concluded. Effect of power coefficient C_p on blade thrust load distribution at advance-diameter ratio J of approximately 2.90 and free-stream Mach number M_o of approximately 0.50. Curtiss 838-1C2-18R1 four-blade propeller.

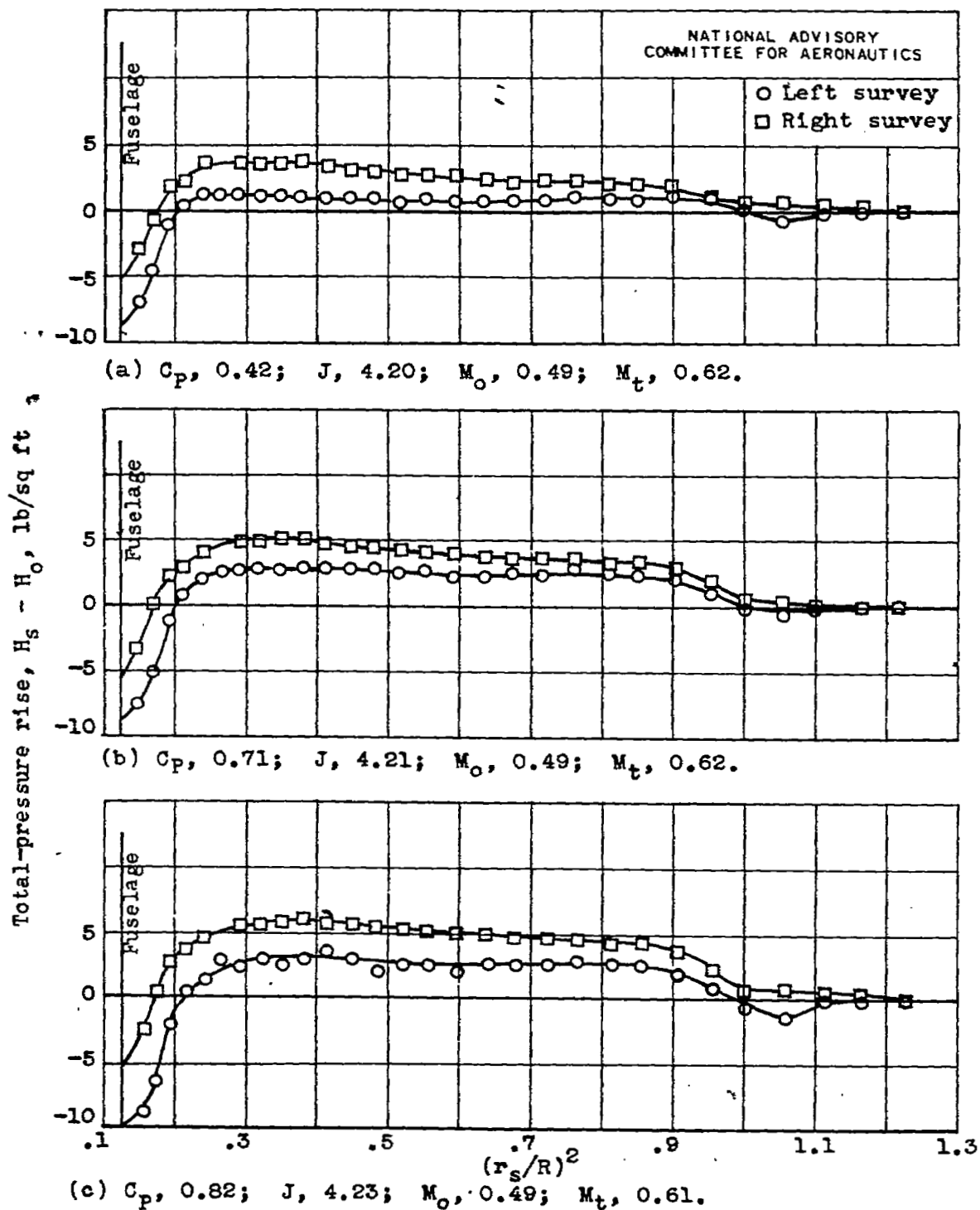


Figure 12.- Effect of power coefficient C_p on propeller efficiency η at advance-diameter ratio J of approximately 4.20 and free-stream Mach number M_o of approximately 0.50. Curtiss 838-1C2-18R1 four-blade propeller.

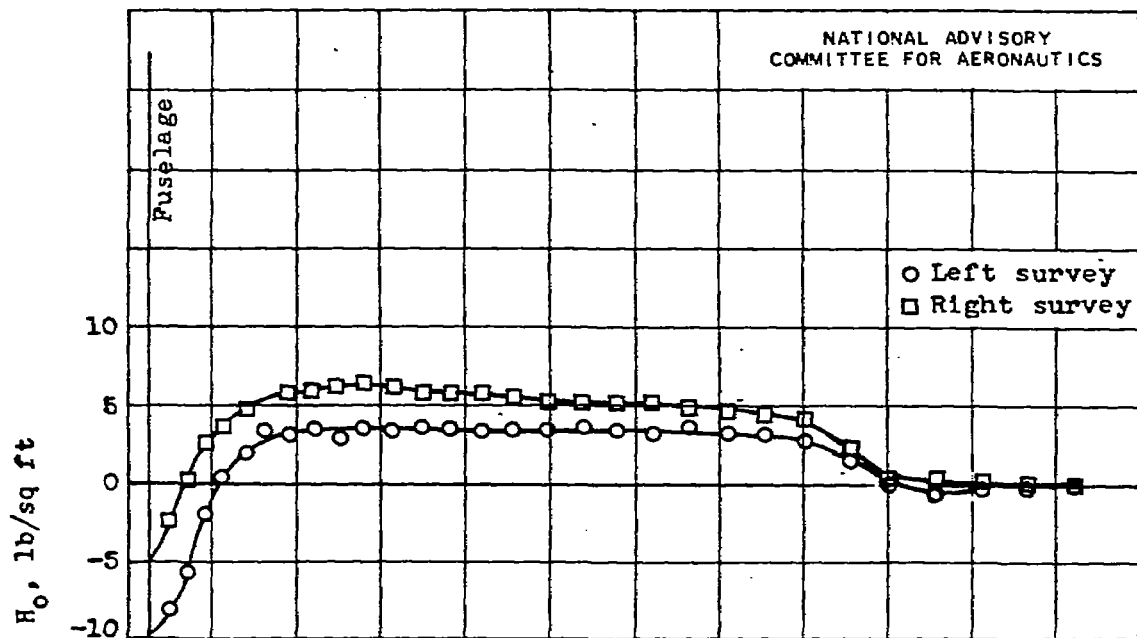
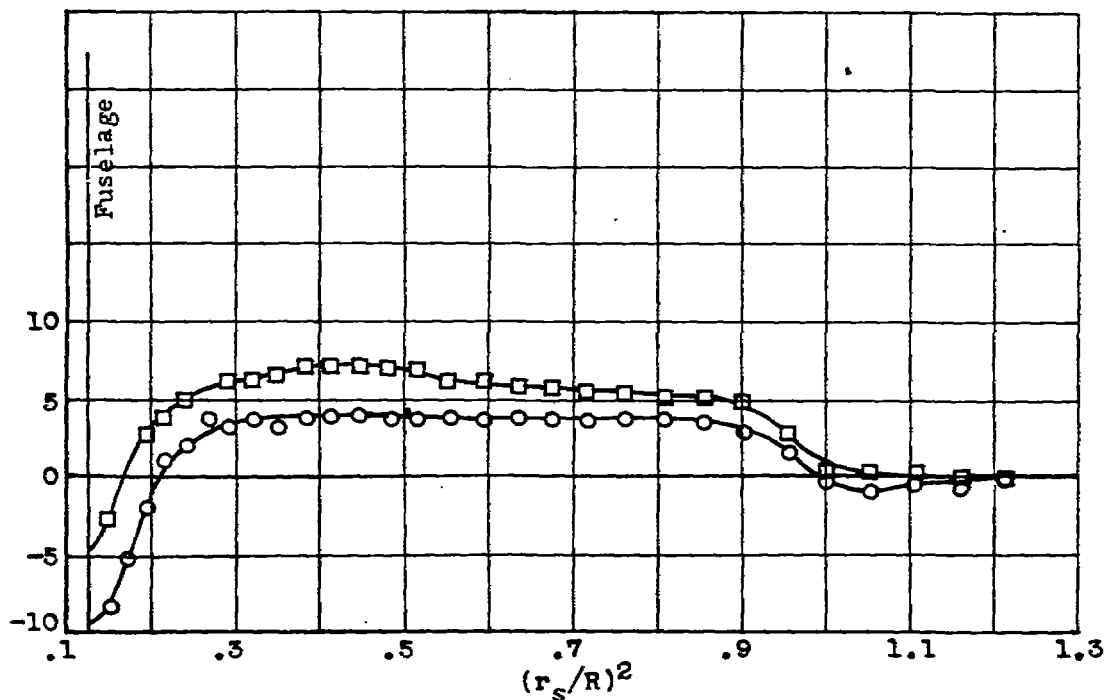
(d) C_p , 0.94; J , 4.23; M_0 , 0.49; M_t , 0.61.(e) C_p , 1.03; J , 4.23; M_0 , 0.49; M_t , 0.62.

Figure 12.- Concluded. Effect of power coefficient C_p on propeller efficiency η at advance-diameter ratio J of approximately 4.20 and free-stream Mach number M_0 of approximately 0.50. Curtiss 838-1C2-18R1 four-blade propeller.

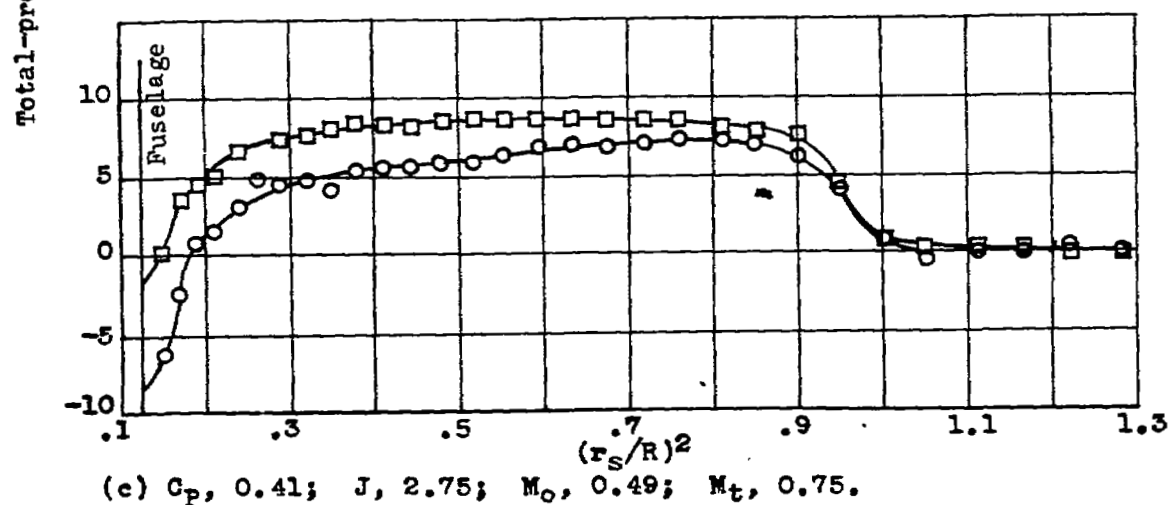
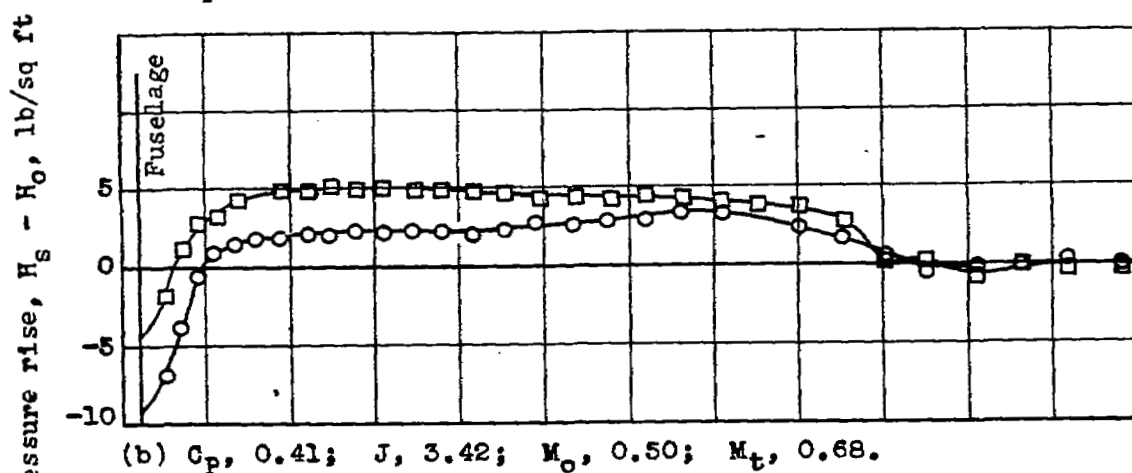
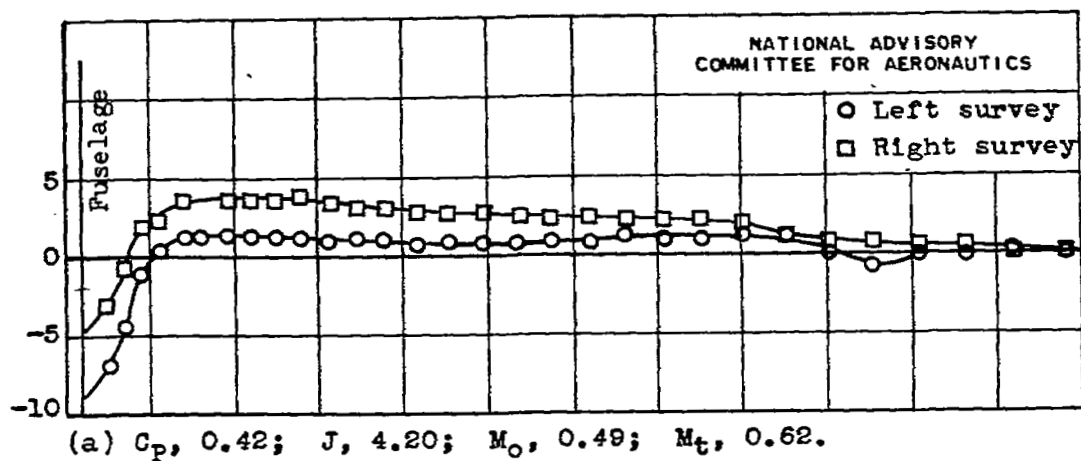
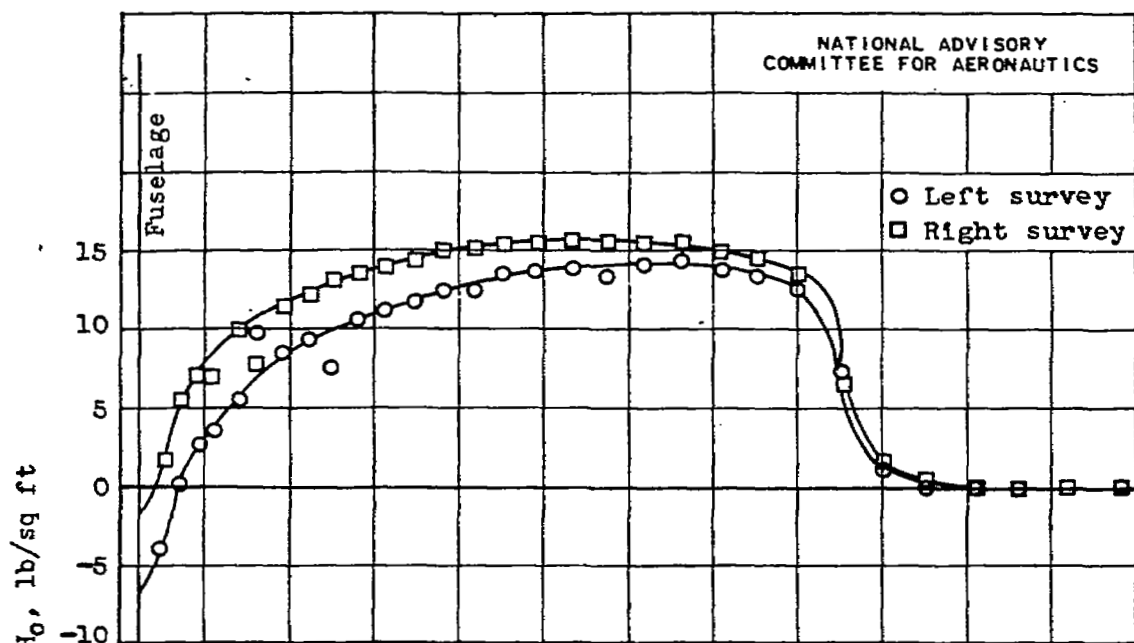
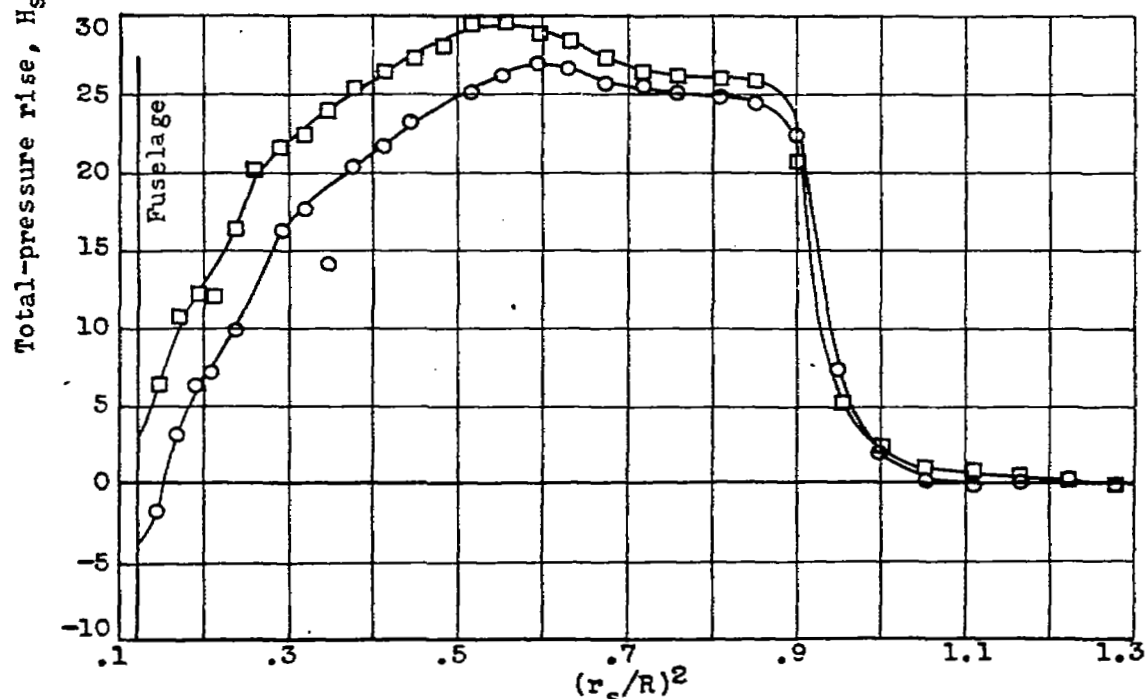


Figure 13.- Effect of advance-diameter ratio J on blade thrust load distribution at power coefficient C_p of approximately 0.40 and free-stream Mach number M_o of approximately 0.50. Curtiss 838-1C2-18R1 four-blade propeller.

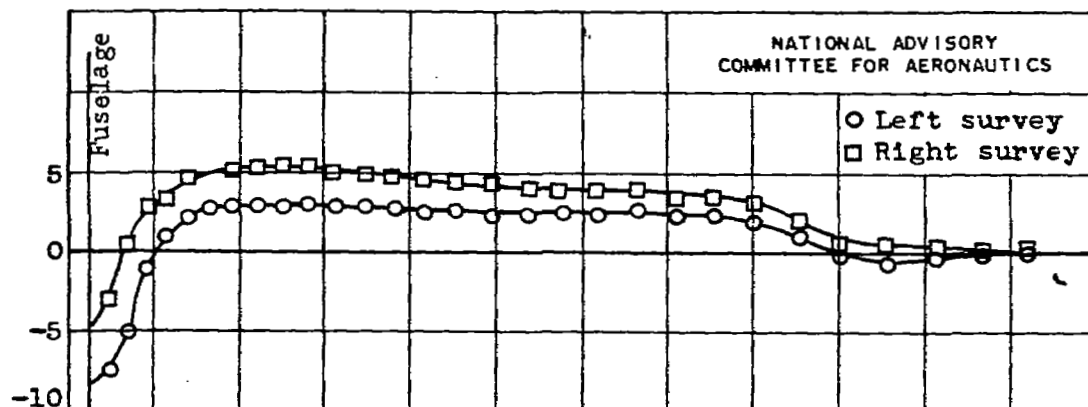


(d) C_p , 0.41; J , 2.20; M_o , 0.49; M_t , 0.86.

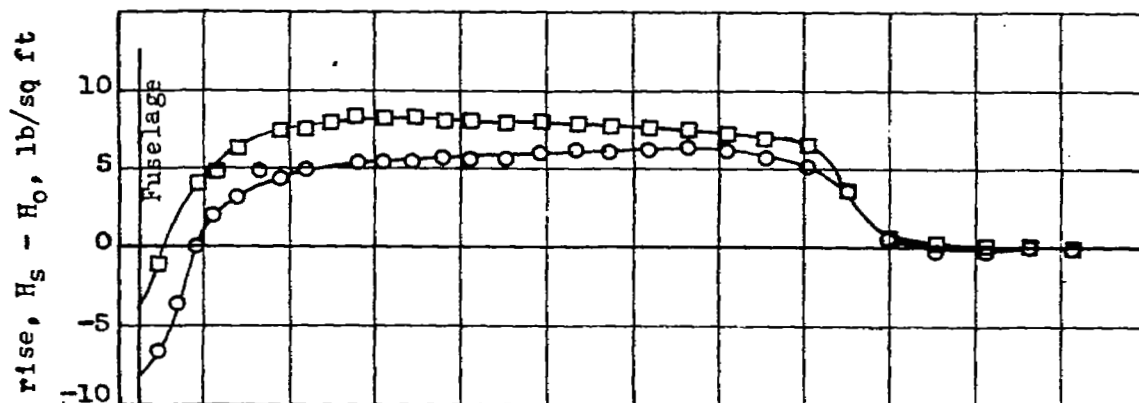


(e) C_p , 0.41; J , 1.75; M_o , 0.49; M_t , 1.01.

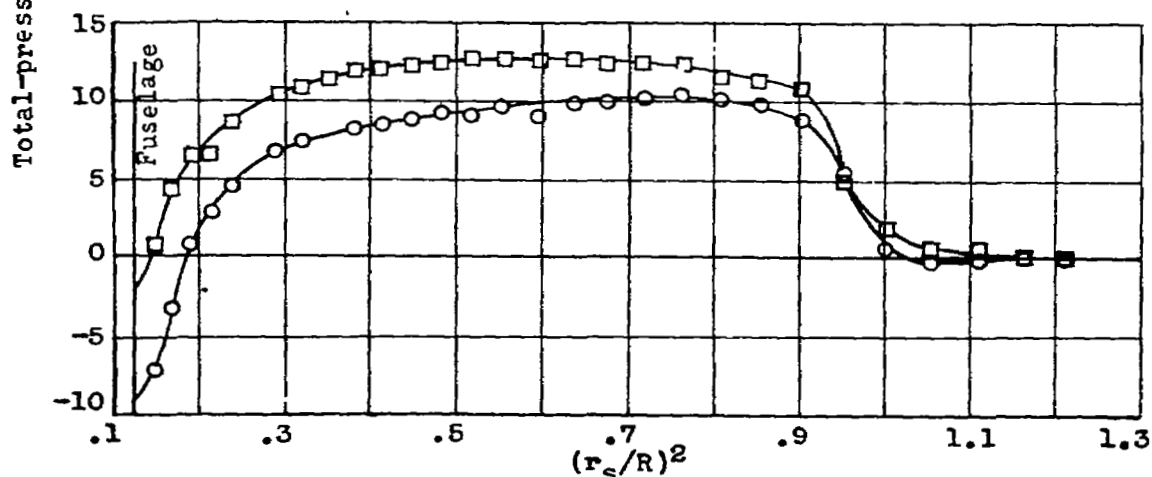
Figure 13.- Concluded. Effect of advance-diameter ratio J on blade thrust load distribution at power coefficient C_p of approximately 0.40 and free-stream Mach number M_o of approximately 0.50. Curtiss 838-1C2-18R1 four-blade propeller.



(a) C_p , 0.71; J , 4.21; M_o , 0.49; M_t , 0.61.



(b) C_p , 0.72; J , 3.43; M_o , 0.50; M_t , 0.68.



(c) C_p , 0.72; J , 2.92; M_o , 0.50; M_t , 0.73.

Figure 14.- Effect of advance-diameter ratio J on blade thrust load distribution at power coefficient C_p of approximately 0.70 and free-stream Mach number M_o of approximately 0.50. Curtiss 838-1C2-18R1 four-blade propeller.

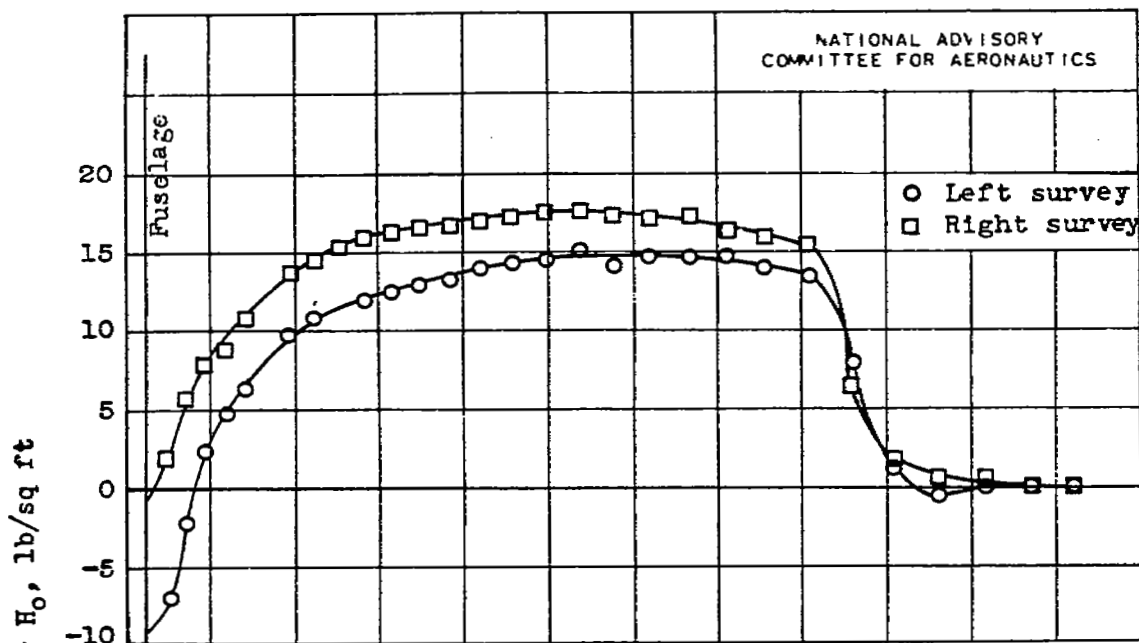
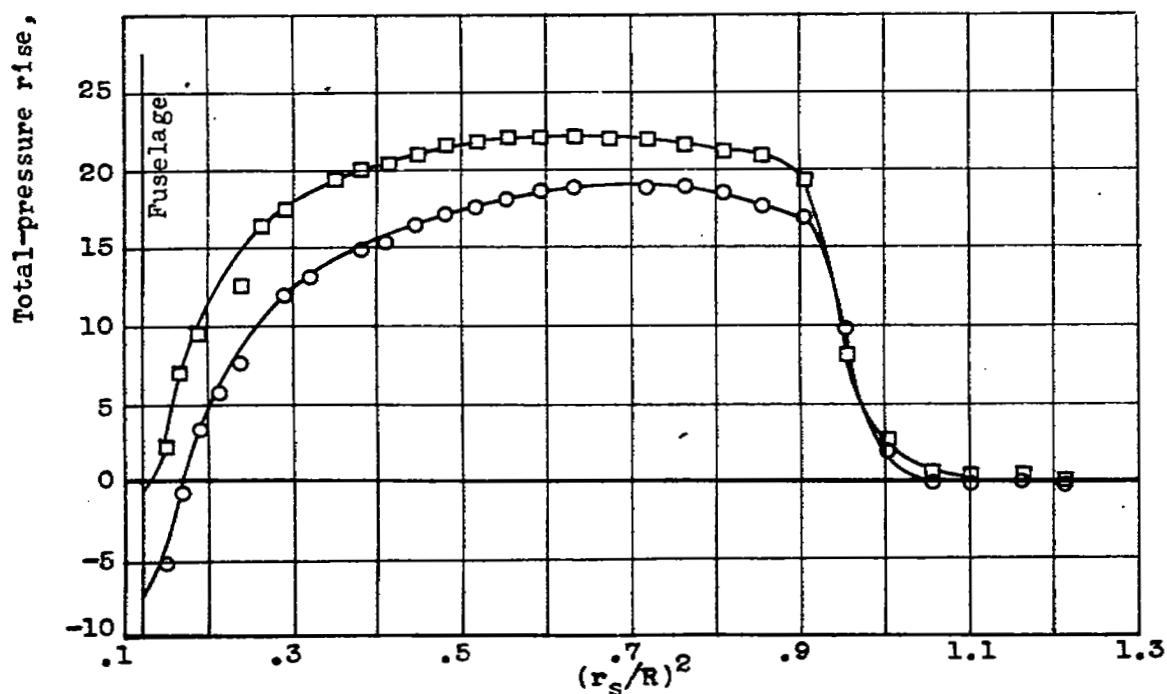
(d) C_p , 0.71; J , 2.59; M_0 , 0.50; M_t , 0.79.(e) C_p , 0.71; J , 2.38; M_0 , 0.50; M_t , 0.82.

Figure 14.- Concluded. Effect of advance-diameter ratio J on blade thrust load distribution at power coefficient C_p of approximately 0.70 and free-stream Mach number M_0 of approximately 0.50. Curtiss 838-1C2-18R1 four-blade propeller.

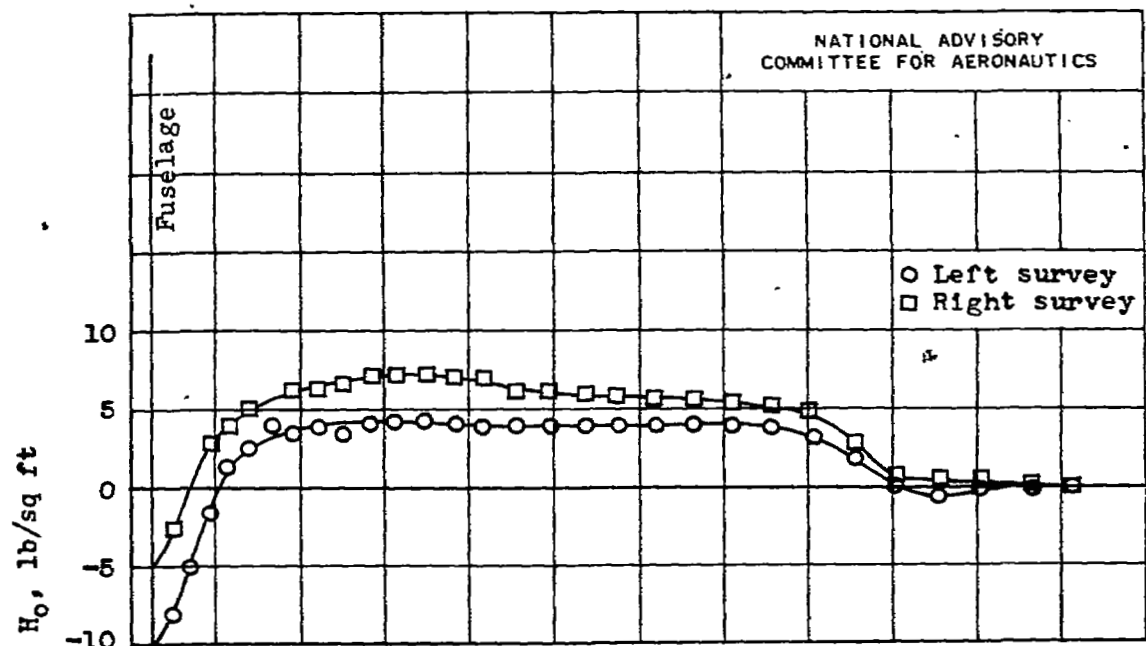
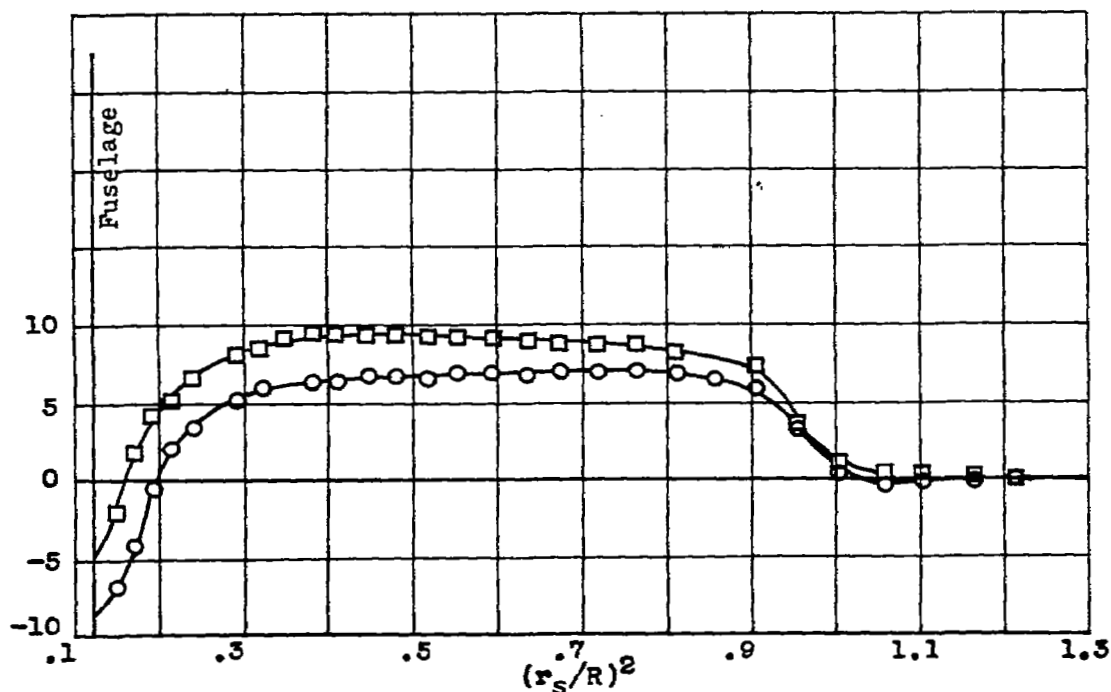
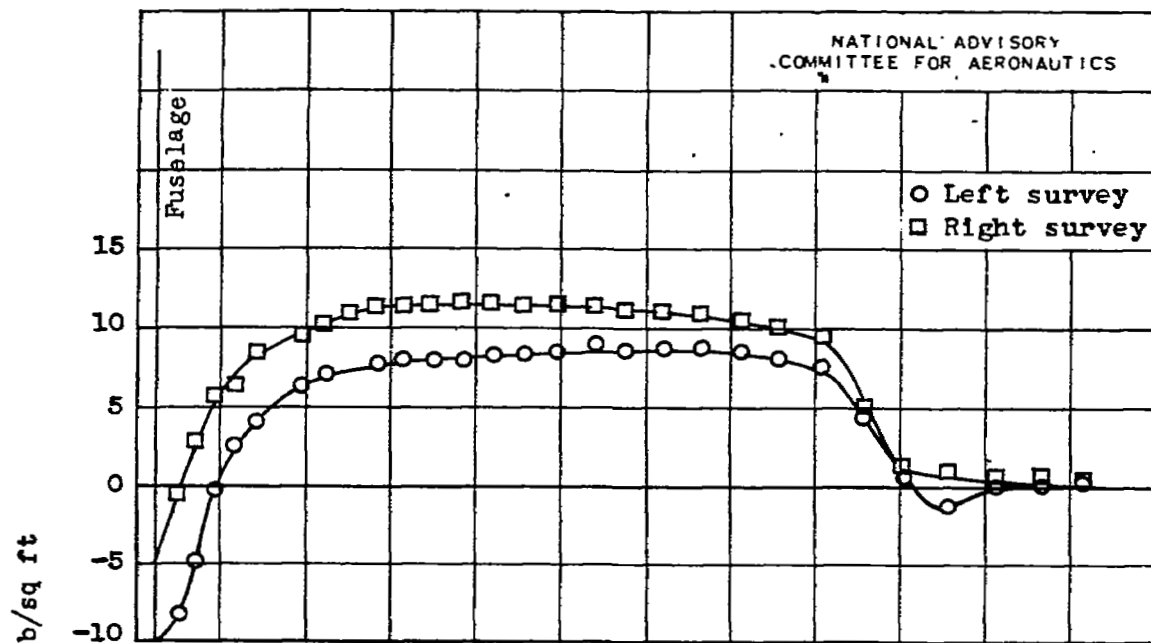
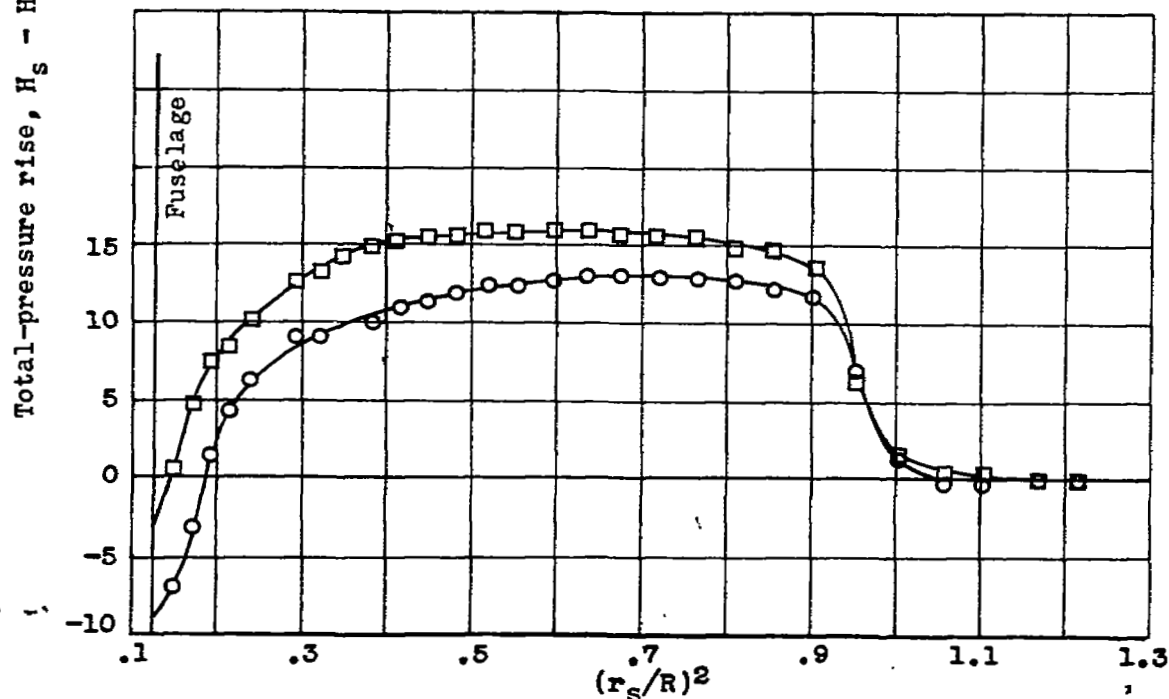
(a) C_p , 1.03; J , 4.23; M_o , 0.49; M_t , 0.62.(b) C_p , 1.03; J , 3.67; M_o , 0.50; M_t , 0.65.

Figure 15.- Effect of advance-diameter ratio J on blade thrust load distribution at power coefficient C_p of approximately 1.00 and free-stream Mach number M_o of approximately 0.50. Curtiss 838-1C2-18R1 four-blade propeller.



(c) C_p , 1.02; J , 3.41; M_o , 0.50; M_t , 0.68.



(d) C_p , 1.02; J , 3.02; M_o , 0.50; M_t , 0.72.

Figure 15.- Concluded. Effect of advance-diameter ratio J on blade thrust load distribution at power coefficient C_p of approximately 1.00 and free-stream Mach number M_o of approximately 0.50. Curtiss 838-102-18R1 four-blade propeller.

